EFFECT OF GPS ERROR SOURCES AND TECHNIQUES TO MITIGATE THEM FOR IMPROVED GPS POSITION FIX

TO7402

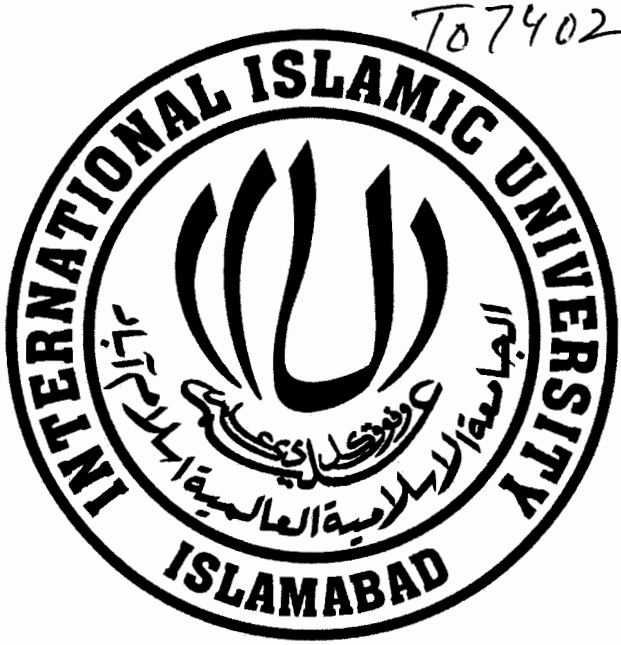

Researcher:
Tahir Saleem
Reg No. 110-FET/MSEE/F07

Supervisor:
Dr. Muhammad Usman

Department of Electronic Engineering

Faculty of Engineering and Technology

INTERNATIONAL ISLAMIC UNIVERSITY, ISLAMABAD

Accession No. TH 7402

MS
629.045
TAE

1- Global positioning system

&

EFFECT OF GPS ERROR SOURCES AND TECHNIQUES TO MITIGATE THEM FOR IMPROVED GPS POSITION FIX

By

Tahir Saleem
Registration No: 110-FET/MSEE/F07

A thesis submitted in partial fulfillment of the requirements for the Degree of Master of Science in Electronic Engineering with specialization in Communication & Signal Processing at the Faculty of Engineering and Technology, International Islamic University Islamabad.

Supervisor **(August, 2010)**
Dr. Muhammad Usman,
Visiting Faculty Member,
International Islamic University Islamabad .

DEDICATED TO

MY

LOVING PARENTS,

TEACHERS AND

FRIENDS

(Acceptance by the Viva Voice Committee)

Title of Thesis: Effect of GPS Error Sources and Techniques to Mitigate them for improved GPS Position Fix

Name of Student: Tahir Saleem

Registration No: 110-FET/MSEE/F07

Accepted by the Faculty of Engineering and Technology, INTERNATIONAL ISLAMIC UNIVERSITY, ISLAMABAD, in partial fulfillment of the requirements for the Master of Science Degree in Electronic Engineering.

External Examiner
Dr. Rab Nawaz
Scientist NESCOM, Islamabad.

Internal Examiner
Dr. Arbab Ali Khan
Associate Professor,
FET, IIU, Islamabad.

Supervisor
Dr. Muhammad Usman
Visiting Faculty Member,
FET, IIU, Islamabad.

Date: 31/08/2010

ABSTRACT

GPS is used for navigation and positioning purposes by a diverse set of users. However the position measured by a commercial GPS receiver is subject to errors from various sources. These sources of errors in GPS navigation (satellite clock, receiver clock, atmospheric and multipath errors) induce biases in the measurement of pseudo range and degrade system accuracy in case of commercial GPS receivers.

In the current research endeavor different error sources and their impact on GPS position accuracy is critically analyzed. Besides this different currently used techniques to reduce these errors for improved GPS positioning are also studied and analyzed. Special emphasis is given to atmospheric errors. In this regard a tropospheric error correction model is simulated on real captured GPS data and results are analyzed.

ACKNOWLEDGEMENTS

I find no word at my command to express my deepest sense of gratitude to the Almighty Allah, the most Merciful and the most Gracious for the blessing bestowed upon and the courage, strength and determination which He has given to me undertake this project.

Secondly I offer special thanks and applause to honorable Personality Dr. Muhammad Usman, my project supervisor and Allied Faculty member of Faculty of Engineering and Technology IIU, Islamabad for his kind guidance, help and valuable consultation throughout the course of this project.

My acknowledgment will remain incomplete if I don't mention the help and companionship of Engr. Aleem Khaliq and Mr. Hammad (Lab Technician at DEE, FET IIUI) for their co-operation during my research work.

I am also thankful to my friend Mr. Muhammad Tahir, who helped me a lot in completing this thesis.

TAHIR SALEEM

FORWARDING SHEET

The thesis entitled Effect of GPS Error Sources and Techniques to Mitigate them for improved GPS Position Fix submitted by Tahir Saleem Registration No: 110-FET/MSEE/F07 in partial fulfillment of the requirements for the Master of Science Degree in Electronic Engineering with specialization in Communication in Signal Processing has been completed under my guidance and supervision. I am satisfied with the quality of student research work and allow him to submit this thesis for further process of as per IIU rules and regulations.

Date: 3/8/10

Signature:

Name: Dr. Muhammad Usman

TABLE OF CONTENTS

Approval sheet iv

Abstract v

Acknowledgements vi

Forwarding Sheet vii

Table of Contents viii

List of Tables xi

List of Figures xii

List of Abbreviations xiii

1.1 Objectives of the Thesis 1

1.2 Organization of the Thesis 1

2.1 The Global Positioning System (GPS) 3

2.1.1 General Overview 3

2.1.2 System Description 4

2.1.2.1 Space Segment 4

2.1.2.2 Control Segment 4

2.1.2.3 User segment 5

2.1.3 GPS Satellite Signals and Data..... 5

2.1.3.1 Carrier 6

2.1.3.2 Navigation Data 6

2.1.3.3 Spreading Sequence 8

2.1.3.3.1 C/A Code..... 8

2.1.3.3.2 P (Y)-Code..... 12

2.1.4 GPS Satellite Signal Modulation 13

2.1.5 GPS Orbits 14
2.1.6 GPS Theory and Principle of Operation 16
2.1.7 GPS Services 17
2.1.7.1 Precise Positioning Service 17
2.1.7.2 Standard Positioning Service 18
2.1.8 GPS OBSERVATIONS 18
2.1.8.1 Pseudorange Measurement: 18
2.1.8.2 Carrier Phase Measurement: 21
2.1.8.3 Doppler Frequency Measurement: 22

3.1 System Wide Sources of Errors 23
3.1.1 Ephemeris/Orbital Error 24
3.1.2 Satellite Clock Errors 25
3.1.3 Atmospheric Errors 26
3.1.3.1 Ionospheric Errors 27
3.1.3.2 Troposphere Errors 28
3.2 Local GPS Error Sources 30
3.2.1 Multipath Errors 31
3.2.2 Satellite Geometry 33
3.2.3 Receiver Noise 34
3.2.4 Receiver Clock Error 35

4.1 Errors Sources 36
4.2 Mitigation Techniques 38

5.1 Capturing of GPS Data 43
5.2 Analysis of GPS Data 44
5.3 Acquisition and Tracking of Satellites 45
5.4 Function Tropo 51

5.5 Position before and after Tropospheric Correction 52

6 Conclusion and Recommendations 56

References **59**

LIST OF TABLES

S/N	Table No	Title of Tables	Page No
1.	2.1	GPS Code Generator Polynomials and Initial States	8
2.	2.2	GPS Ephemeris Data Definitions	15
3.	3.1	GPS Ranging Errors	24
4.	3.2	Tropospheric Delay on Measured Range	29
5.	3.3	Local GPS Error Sources	31
6.	3.4	GPS Errors	35
7.	5.1	Description of Acquisition Specific Variable	46
8.	5.2	Description of Important Parameters	49
9.	5.3	Description of Important Parameters of Tropo Function	50
10.	5.4	Comparison of Results Obtained for Position Calculations before and after tropospheric correction	51

LIST OF FIGURES

S/N	Figure No	Title of Figures	Page No
1.	2.1	The GPS Signal Spectrum	5
2.	2.2	GPS Navigation Data Structure	7
3.	2.3	C/A Code Generator	8
4.	2.4	Auto-Correlation Function	11
5.	2.5	The Autocorrelation Function of C/A Code (Matlab Diagram)	11
6.	2.6	GPS Satellite Signal Structure	13
7.	2.7	GPS Code Mixing with Data	14
8.	2.8	Definition of the User to Satellite Vector r	20
9.	3.1	System wide Errors and their Impact	23
10.	3.2	Multipath Effect	32
11.	3.3	Comparison of High and Small DOP	33
12.	5.1	Time and Frequency Domain Plot for actual GPS Data	44
13.	5.2	Acquisition Result	45
14.	5.3	Tracking Results for Channel 2	47
15.	5.4	Tracking Results for Channel 4	48
16.	5.5	East Coordinate variations with and without Tropospheric Correction	53
17.	5.6	North Coordinate variations with and without Tropospheric correction	53
18.	5.7	Uping Coordinate variations with and without Tropospheric correction	54
19.	5.8	Position before Troposphere correction	55
20.	5.9	Position after Troposphere correction	55
21.	5.10	Satellite Sky Plot	57

LIST OF ABBREVIATIONS

ANN	Artificial Neural Network
C/A	Carrier Acquisition
CDMA	Code Division Multiple Access
DGPS	Differential Global Positioning System
DLL	Delay Lock Loop
DOP	Dilution of Precision
DSSS	Direct Sequence Spread Spectrum
FM	Frequency Modulation
FFT	Fast Fourier Transform
GNSS	Global Navigation Satellite Systems
GPS	Global Positioning System
IF	Intermediate Frequency
IFFT	Inverse Fast Fourier Transform
DFT	Discrete Fourier Transform
LEO	Low Earth Orbit
LMS	Least-Mean-Square
LO	Local Oscillator
NAV	Navigation
PLL	Phase Lock Loop
PRN	Pseudorandom Number
PSD	Power Spectral Density
Q	Quadrature
RF	Radio Frequency
UTM	Universal Transverse Mercator Grid System

CHAPTER 1 INTRODUCTION

1.1 Objective of the Thesis

There are two major objectives of the thesis. First one is to assess the impacts of the different error sources on GPS positioning. These errors include the orbits inaccuracies, satellite and receiver clocks drift, the ionosphere and troposphere delay, multipath, and receiver noise. Each of these errors is investigated thoroughly and also the currently used techniques to mitigate these errors are explored.

The second objective is how to apply the different techniques used to mitigate the errors developed up till now in order to obtain an improved GPS navigation solution. Special focus was kept on Differential GPS and methods to remove and/or mitigate the atmospheric errors. In this regard a correction modal for the error caused by the troposphere is simulated on actual acquired GPS data and results were analyzed and recorded in the Simulation and Comparison of Results chapter of this thesis.

1.2 Organization of the Thesis

The thesis consists of six chapters. The brief description of these remaining chapters is as follows.

In order to understand the error sources of GPS it is imperative to be familiar with the fundamentals of GPS. In this regard Chapter 2 starts with an introduction of GPS, including a description of the three constituent parts, namely, the control segment, the

space segment, and the user segment. The GPS signal is described in detail and the services provided by the GPS are also discussed.

Chapter 3 commences with a diagram which shows some of the important error sources and their impacts. In the remaining part each category of error is further elaborated in detail.

Chapter 4 is reserved to discuss the research work being carried out in the exciting field of GPS accuracy by contemporary researchers and authors. Different methods and models devised by various researchers are highlighted and their potential to mitigate GPS errors is also elaborated.

Chapter 5 presents the simulation work performed in Matlab and the results obtained. It also depicts different diagrams obtained in Matlab, when the actual captured GPS data, was analyzed. The results are compared, findings are discussed and any shortcomings are analyzed.

Chapter 6 provides the conclusions and recommendations for future research.

CHAPTER 2 BRIEF DESCRIPTION OF GPS

2.1 The Global Positioning System (GPS)

2.1.1 General Overview

The Global Positioning System (GPS) is a U.S. space-based global navigation satellite system maintained by U.S Department of Defense. The GPS, formally called NAVSTAR (Navigation Satellite Timing and Ranging) GPS by the U.S Department of Defense was basically developed for U.S military as a military navigating system for guiding missiles, ships and aircrafts towards their targets. The GPS evolved from four previous satellite systems: transit, a U.S. Navy system developed by Johns Hopkins Applied Research Lab; Timation, developed at the Naval Research Lab; Project 621B, an Air Force Study Program; and the Defense Navigation Satellite System. It was researched in the 1960s and was officially established as a program in 1969 and approved for development in December 1973. The first satellite was launched in February of 1978, and the entire constellation of 24 satellites was completed in December 1993. All system components reached full operational capability in the spring of 1995.

Due to the tremendous accuracy potential of this system, and the latest improvements in receiver technology, the GPS (Global Positioning Systems) has revolutionized navigation and position location for more than a decade [1]. GPS works in any weather conditions, anywhere in the world, 24 hours a day. There are no subscription fees or setup charges to use commercial GPS services.

2.1.2 System Description

The GPS consist of the following three major segments, which are explained below: -

2.1.2.1 Space Segment

There are a total of 32 GPS satellites in GPS Space Segment in which 24 satellites are currently operational divided into six orbits and each orbit has four satellites. Each orbit makes a 55-degree angle with the equator, which is referred to as the inclination angle. The orbits are separated by 60 degrees to cover the complete 360 degrees. The satellites have an average orbit altitude of 20,200 km above the surface of earth and complete one orbit in approximately 11 hours and 58 minutes. The system is designed so that at least five satellites are visible at any point on the earth's surface having a clear view of the sky. These satellites are travelling at speed of roughly 11,265 km (7,000 miles) per hour. They are constantly moving, making two complete orbits in less than 24 hours. The constellation is constantly being replaced and upgraded and some of the satellites are kept as spare for emergency situations.

2.1.2.2 Control Segment

The Control Segment primarily consists of a Master Control Station (MCS) at Falcon Air Force Base (AFB) in Colorado Springs, USA as well as Six Monitor Stations (MS) and Four Ground Antennas (GA) at various locations around the world. The monitor stations are located at Falcon AFB, Hawaii, Kwajalein, Diego Garcia and

Ascension islands. The MCS is the central processing facility for the Control Segment and is responsible for monitoring and managing the satellite constellation.

2.1.2.3 User Segment

The User Segment is the ultimate segment in the chain of system components. It is the GPS receiver, consisting of an antenna, signal tracking circuitry, user interface, power, and a microprocessor to control the operation of the receiver. There are many receivers now commercially available ranging from low-cost, single-frequency sets to expensive dual-frequency devices.

2.1.3 GPS Satellite Signals and Data

GPS signals are transmitted on two radio frequencies in the UHF band. These frequencies are respectively known as L1 with frequency 1575.42 MHz and L2 having frequency 1227.60 MHz. The UHF band ranges from 500MHz to 3GHz in the frequency band. The spectrum of the GPS signal is shown in figure 2.1 below.

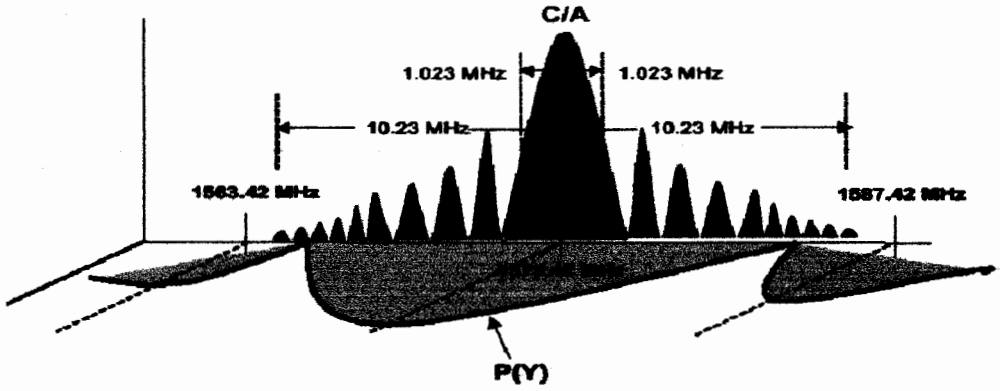

Figure 2.1 The GPS Signal Spectrum

The GPS signals consist of the following three parts which are described in detail below [2].

2.1.3.1 Carrier

The carrier wave with frequency L1 or L2 and which carries information from satellite to GPS receiver.

2.1.3.2 Navigation Data

This part of GPS signal contains information about satellite orbits. This information is uploaded by the ground stations in the GPS Control Segment to all satellites with bit rate of 50 bps. The navigation message contains vast amount of information that is used by GPS receivers to optimize the acquisition of satellite signals and calculate user's position. The navigation message includes data unique to the transmitting satellite as well as data common to all satellites.

The navigation data are transmitted on the L1 frequency which is superimposed on both the P (Y) code and the C/A code which will be discussed in the next subsection. In the generic GPS receiver the navigation message is extracted by a 50 bps BPSK demodulator that follows the C/A code correlator. The narrow bandwidth of the navigation message ensures a high SNR ratio at the demodulator input and correspondingly low probability of bit errors in the navigation message [2]. The navigation message consists of 25 frames of data with each frame consisting of 1,500 bits. Each frame contains 5 subframes, each having length 300 bits. Further each subframe composed of 10 words, where each word having length 30 bits. However,

some information is contained in the sequence of frames, and the complete data set requires 12.5 minutes for transmission. The most important elements of the message are repeated in every frame. Figure 2.2 depicts the overall structure of an entire navigation message.

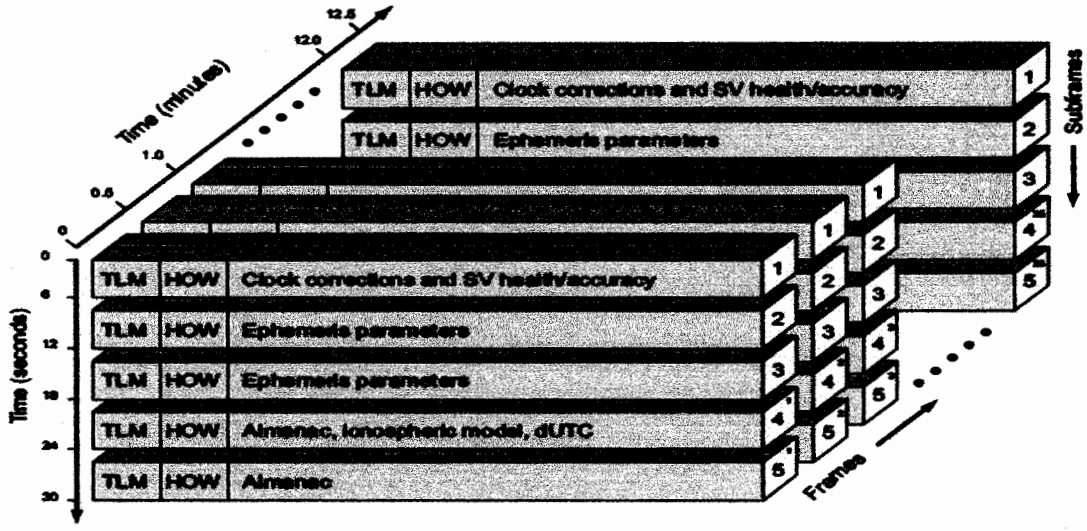

Figure 2.2 GPS Navigation Data Structure

2.1.3.3 Spreading Sequence

Each satellite has two unique spreading sequences or codes. The first one is the C/A (Coarse Acquisition) code, while the other one is known as precision code (P(Y)) [3].

2.1.3.3.1 C/A Code

The C/A (Course-Acquisition) codes are also known as Pseudo-random noise sequences, or simply PRN sequences. The C/A code consists of 1023 bits out of which 512 are ones and 511 are zero distributed at random. As explained on the next page PRN

sequence is pseudorandom not random because its generation is entirely deterministic [3]. The sequence has a chipping rate of 1.023 MHz that repeats every 1 millisecond. A different PRN code is assigned to each GPS satellite which is selected from a unique family of sequences known as Gold codes, described by Robert Gold in 1967. The Gold codes have been chosen as they have very good autocorrelation and low cross correlation properties which can used in signal detection. They are specific sequences of pseudorandom numbers and can be generated using two tapped linear feedback shift registers (LFSR). The two 10 bit shift registers are called G1 and G2 and generate the maximum length pseudo noise (PN) codes with a length of $2^{10} - 1 = 1{,}023$ bits. The C/A code generator circuit in block diagram form is shown in figure 2.3. The polynomial and initial state for the C/A code are as follows: -

C/A Code G1	$1 + X^3 + X^{10}$	11111111111
C/A Code G2	$1 + X^2 + X^3 + X^6 + X^8 + X^9 + X^{10}$	11111111111

Table 2.1 GPS Code Generator Polynomials and Initial States

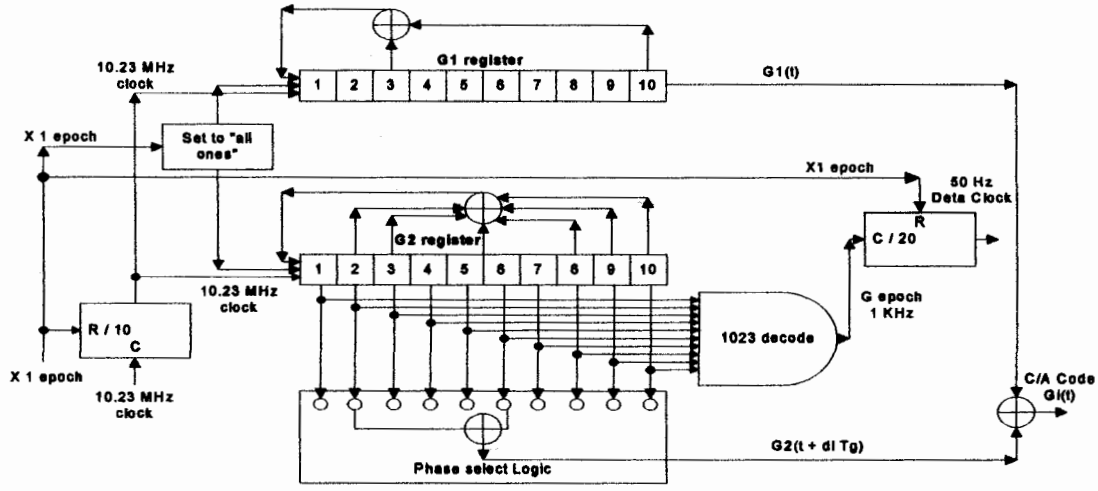

Figure 2.3 C/A Code Generator

As evident from figure 2.3 the unique code for each SV (Space Vehical) is the result of exclusive-OR of a delayed version of G2 output sequence and the G1 direct output sequence. The C/A-code is transmitted only on L1 and is not encrypted and is therefore available to all GPS users. Employing the exclusive-OR of two maximum length shift registers, as shown above; there are 1023 possible gold codes for the GPS C/A code generator architecture. But not all the sequences have low cross correlation properties. Therefore, only 37 Gold codes with the best possible properties have been selected for the GPS space segment. Low cross-correlation of the sequence is imperative because the GPS receiver has to distinguish between signals from as many as 12 satellites at the same time using correlation techniques.

2.1.3.3.1.1 Correlation Properties of C/A code

Correlation is the product integration of received signal with the replica of transmitted waveform. Fundamentally, correlation is a statistical process and is essentially the measure of similarity. The correlation characteristics are used for the optimum detection of signals in white noise and are particularly important in the detection of GPS signals that are buried in noise. This property is used in the receiver to determine the propagation time by correlating the received signal with an internally generated copy of the transmitted signal. The time shift for the highest correlation is a measure of the propagation time.

One of the most important properties of the C/A codes is their high autocorrelation peak and low cross-correlation. However, in order to detect the presence of a weak signal, the peak of the autocorrelation of the weak signal must be stronger than the cross-

correlation peaks of the strong signals. Theoretically if the codes are orthogonal, the cross correlation values will be zero. However, the Gold codes are only near orthogonal codes, so the cross correlation values of the C/A codes are not zero but rather have small values.

Auto-correlation means the multiplication and integration of the signal with the delayed version of itself. The auto correlations characteristics of the GPS PRN codes are fundamental to the signal demodulation process [1]. The general formula for auto correlation function (ACF) is defined as: -

$$R1(\tau) = \int_{-\infty}^{\infty} f1(t) f1(t+\tau)\, dt \tag{2.1}$$

Where τ = the phase shift of the replica function.

The GPS uses codes that have similar auto-correlation and power spectrum properties as the random binary codes, but the GPS codes are deterministic, periodic, and predictable and are easily reproduced by suitably equipped receivers. The auto correlation function of a maximum length PRN sequence is an infinite series of triangular functions, with the peaks depicting the value of maximum correlation and have period of NTC seconds as shown in figure 2.4. Mathematically ACF for C/A can be defined as: -

$$RG(\tau) = \frac{1}{1023 T_{CA}} \int_{t=0}^{t=1023} Gi(t)\, Gi(t+\tau)\, dt \tag{2.2}$$

Where Gi(t) = C/A code Gold code sequence as a function of time t for i^{th} SV.

TCA = C/A code chipping period (977.5 n sec) and τ = phase of the time shift in the autocorrelation function RG (τ)

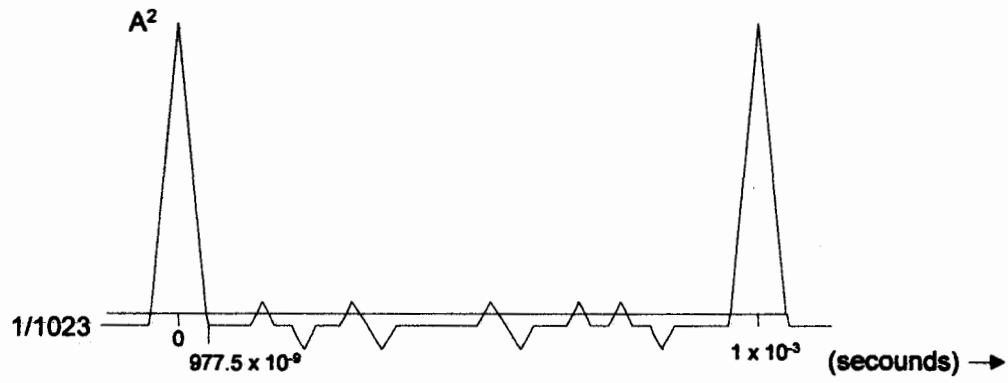

Figure 2.4 Auto-Correlation Function

In Figure 2.5 the autocorrelation of one set of C/A code for a satellite is plotted in Matlab environment. The maximum autocorrelation value is 1023, which corresponds to the number of chips in one set of the C/A code.

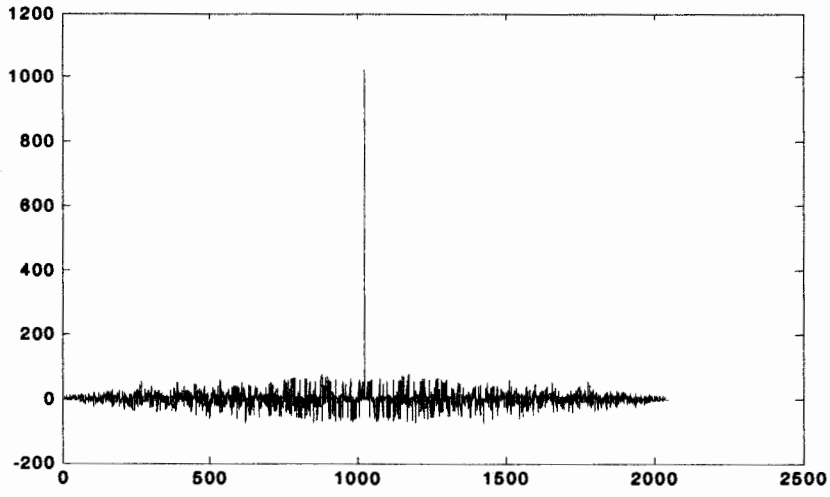

Figure 2.5 The Autocorrelation of C/A code (Matlab Diagram)

The cross-correlation values between two C/A Codes are very small; hence the GPS satellites can simultaneously broadcast signals at the same frequency. This property makes it easy to find out when two similar codes are perfectly matched. From Figure 2.5

it can be seen that the correlation peak value is much more significant than other correlation values. The high peak value helps the receiver to acquire the GPS signal. The secondary peaks in the autocorrelation are at least approximately 24 dB lower than the higher peaks. When the receiver code phase aligns with the incoming signal code phase, there is a +30 dB improvement in the SNR.

2.1.3.3.2 P (Y)-Code

The P (Precise) code is a 10.23 MHz PRN code sequence that is 267 days in length. But the P code is normally encrypted and available only to authorized users. Once encrypted, the P code is known as the Y code. It is modulated onto both L1 and L2 carrier. The P(Y) code is generated by the same principle as C/A code, except 4 shift register having 12 cells each are used. However, it will not be discussed further as it is beyond the scope of this project.

2.1.4 GPS Satellite Signal Modulation

The satellite signal structure is explained with the aid of a block diagram as shown in figure 2.6 [1]. The L1 frequency (154 x fo) is modulated by both C/A code and P(Y) code and the navigation message data, whereas the L2 frequency (120 x fo) is modulated by only the P(Y) code and the navigation message data. The frequency fo is called the nominal reference frequency and is equal to 10.23 MHz. Both the C/A codes and P(Y) codes as well as the L1 and L2 frequencies are subjected to the encrypted dither frequency of SA. The SA is used to limit the GPS accuracy for C/A code users and hence cannot be corrected by SPS users as explained in section 2.1.6; however it can be removed by PPS users also explained in section in 2.1.6.

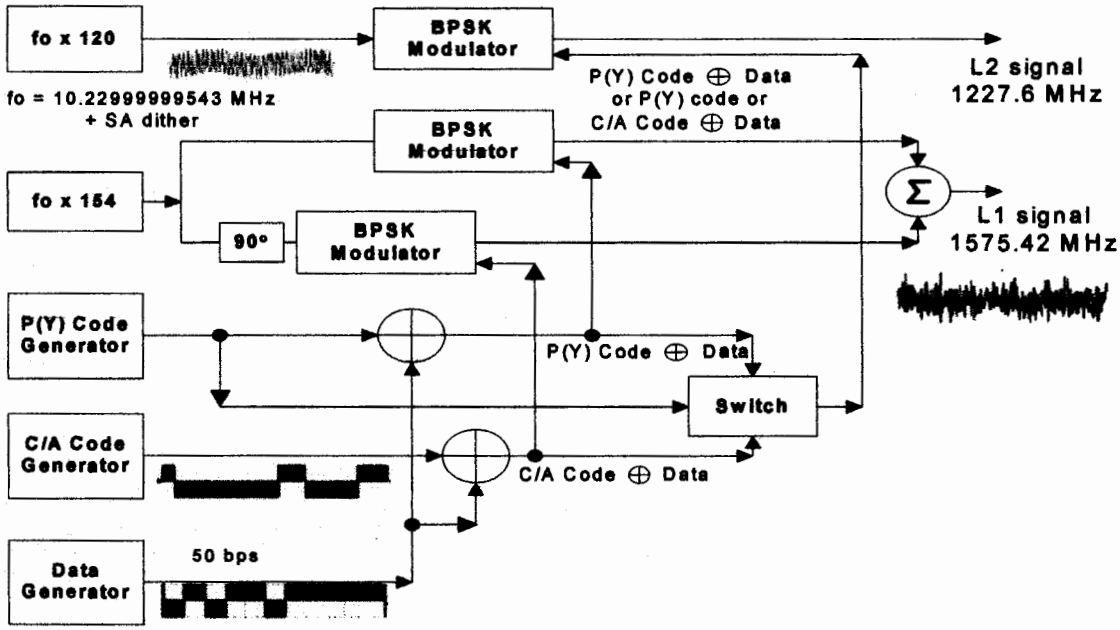

Figure 2.6 GPS Satellite Signal Structure

As evident from the above-mentioned block diagram the 50 bits per second (bps) data is combined with both the C/A code and the P(Y) code prior to modulation with the L1 carrier. The combination is performed by an exclusive-OR process denoted by ⊕ and the modulation is based on the Bi-phase Shift Keying (BPSK) method. The P (Y) code ⊕ data is modulated in phase quadrature with the C/A code ⊕ data on the L1 frequency. Figure 2.7 illustrates the method of C/A code ⊕ data and clarifies that the exclusive OR process is equivalent to binary multiplication of two one bit values. The BPSK technique reverses the carrier phase when the modulating code changes from logic 0 to 1 or 1 to 0. The C/A-code spreads the L1 signal power over a 2.046 MHz bandwidth centered at 1575.42 MHz.

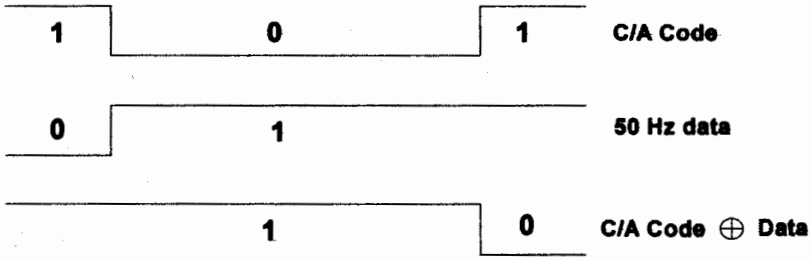

Figure 2.7 GPS Code Mixing with Data

2.1.5 GPS Orbits

A GPS user needs accurate information about the positions of the GPS satellites in order to determine its position. Therefore, it is important to understand the characterization of GPS orbits. The orbital parameters of a satellite are represented by various methods. The GPS ephemeris message not only includes the six orbital parameters but also the time of their applicability and a characterization of how they change over time. With this information the GPS receiver can compute the corrected integral of motion for the SV in order to solve the navigation problem. The following table defines the orbital elements that are used in the algorithms by which a GPS receiver computes the position vector of a satellite (xs, ys, zs) in the ECEF coordinate system, these parameters will be further discussed in the simulation section. Three of the elements define the shape of satellite orbits, whereas three define orientation of the orbit in ECEF coordinate system.

1.	*toe*	Reference time of ephemeris
2.	$\sqrt{a}$	Square root of semi-major axis
3.	*e*	Eccentricity
4.	*Io*	Inclination angle (at time *toe*)
5.	Ωo	Longitude of the ascending node (at weekly epoch)
6.	*Ω*	Argument of perigee (at time *toe*)
7.	Mo	Mean anomaly (at time *toe*)
8.	*di/dt*	Rate of change of inclination angle
9.	Ω	Rate of change of longitude of the ascending node
10.	Δ*n*	Mean motion correction
11.	C_{uc}	Amplitude of cosine correction to argument of latitude
12.	C_{us}	Amplitude of sine correction to argument of latitude
13.	C_{rc}	Amplitude of cosine correction to orbital radius
14.	C_{rs}	Amplitude of sine correction to orbital radius
15.	C_{ic}	Amplitude of cosine correction to inclination angle
16.	C_{is}	Amplitude of sine correction to inclination angle

Table 2.2 GPS Ephemeris Data Definitions

In case of GPS satellites, the orbits are nearly circular with eccentricities of no larger than 0.02 and semi-major axes of approximately 26,560 km. The remaining orbital parameters vary between satellites so that the constellation provides nearly uniform coverage of the entire earth.

GPS almanac data and ephemeris data transmitted by the satellites also include the osculating Keplerian orbital elements. The Keplerian orbital elements in the GPS ephemeris message are augmented by "correction parameters" that allow the user to estimate the Keplerian elements fairly accurately during the periods of time between updates of the satellite's ephemeris message. In order to carry out necessary computation it is important to know the rotation rate of the Earth. According to WGS-84, this rotation rate is $\Omega e = 7.2921151467 \times 10^{-5}$ rad/sec.

2.1.6 GPS Theory and Principle of Operation

The GPS SV broadcasts two carrier frequencies called L1, the primary frequency at 1575.42 MHz, and L2, the secondary frequency at 1227.6 MHz. The satellite signals are transmitted using direct sequence spread spectrum (DSSS) techniques, employing two different ranging codes used as spreading functions as explained in the section 2.1.3.3. These codes broadcasted by the satellites enable a GPS receiver to measure the transit time of the signals and thereby determine the distance between a satellite and the user. The navigation message provides data to calculate the position of each satellite at the time of signal transmission. From this information, the user position coordinates and the user clock offset are calculated using simultaneous equations. Four satellites are normally required to be simultaneously in view for the receiver to solve the equations for three-dimensional (Latitude, Longitude, Altitude) positioning purposes while three satellites are necessary for two dimensional (Latitude, Longitude) positions [4].

Each GPS satellite carries several high accuracy atomic clocks and transmits codes that start at precisely known time. In order to make measurements the GPS employs the concept of time-of-arrival (TOA) ranging to determine user's position. Measurement is made to calculate the time it takes for a signal transmitted by the SV at a known location to reach a user's receiver. By measuring the propagation time of signals broadcasted from multiple SVs at known locations, the receiver can determine its position. Thus the position of GPS receiver is calculated by trilateration, which is the traditional, simplest and most accurate method of locating an unknown position from three points. So at least three satellites are required to compute receiver position.

To formulate the mathematics of the satellite navigation problem, it is necessary to choose a reference coordinate system in which the states of both the satellite and the receiver can be represented. For the purposes of measuring and determining the orbits of the GPS satellites the Earth Centered Inertial (ECI) coordinate system is utilized in which the origin is at the center of mass of the Earth. However for the purpose of computing the position of a GPS receiver, it is more convenient to use a coordinate system that rotates with the earth, this system is known as an Earth Centered Earth Fixed (ECEF) system. In ECEF system, it is easier to compute the latitude, longitude and height parameters which are displayed by the receiver. Latitude is the distance to North or South from Equator; longitude is the distance to East or West from Greenwich city and height is distance from earth surface. It has its x-y plane coincident with the Earth's equatorial plane. In order to carry out the required transformation, it is necessary to have a physical model describing the Earth. The standard physical model of the Earth used for GPS application is DOD's World Geodetic System 1984 (WGS - 84). It is a state-of-the-art global geodetic reference system and depicts an ellipsoidal model of the Earth's shape.

2.1.7 GPS Services

According to the Federal Radionavigation Plan the GPS furnishes two levels of service, the Precise Positioning Service (PPS) and the Standard Positioning Service (SPS) [5].

2.1.7.1 Precise Positioning Service

The PPS is an accurate positioning, velocity and timing service that is available only to authorized users with cryptographic equipment and keys and specially equipped

receivers. The PPS is primarily intended for military purposes. Access to the PPS is controlled by two features using cryptographic techniques i.e. Selective Availability (SA) and Anti-Spoofing (AS). Maximum GPS accuracy is obtained using the P (Y)-code that is transmitted on both L1 and L2 Frequencies. U. S. and Allied military, certain U. S. Government agencies, and selected civil users specifically approved by the U. S. Government, can use the PPS.

2.1.7.2 Standard Positioning Service

The SPS is a less accurate positioning and timing service that is available to all GPS users and is primarily intended for civilian purposes. Civil users worldwide use the SPS without charge or restrictions.

2.1.8 GPS Observations

Three different types of measurements can be obtained when tracking a GPS satellite: pseudorange measurement, carrier phase measurement, and instantaneous Doppler measurement.

2.1.8.1 Pseudorange Measurement:

GPS satellites transmit signals which are labeled with the time of transmission given in the GPS time frame. Receivers measure the time of reception of the signal relative to the receiver clock. If the receiver clock is fully synchronized to GPS time, then the time difference between the transmission time and the reception time is exactly the travel time of the signal. Due to the fact that the satellite and receiver docks are usually

not synchronized, the range determined with this procedure is affected by clock synchronization error therefore it is referred as pseudorange.

The basic pseudorange measurement equation can be given as [6]:

$$p = r + r_d + c\,(d_{\Delta t} - d_{\Delta T}) + ion_d + trop_d + p_\varepsilon \qquad (2.3)$$

Where:

p	measured pseudorange (m),
r	geometric range (m),
rd	orbital error (m),
c	speed of light (m/s),
$d_{\Delta t}$	satellite clock error (s),
$d_{\Delta T}$	receiver clock error (s),
ion_d	ionospheric error (m),
$trop_d$	tropospheric error (m), and
p_ε	receiver code noise plus multipath (m).

As mentioned earlier the signals transmitted by the satellites are used to measure the Time of Arrival (TOA) at the receiver. Since the propagation speed (the speed of light) is known, the distance (geometric range) can be calculated from the delay.

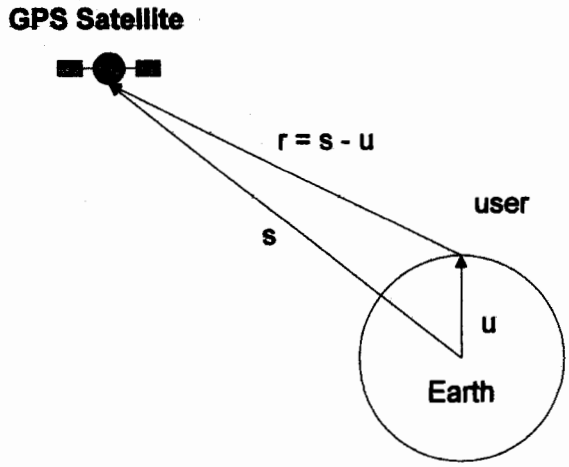

Figure 2.8 Definition of the User-to-Satellite Vector r.

The position of the satellite, s, is known from satellite ephemeris data broadcasts (ECEF coordinates). If a user is located at position u, the user-to-satellite vector r can then be written as shown in Figure 2.8:

$$\mathbf{r} = \mathbf{s} - \mathbf{u} \tag{2.4}$$

Let r represent the distance between a satellite and the user,

$$r = ||\mathbf{r}|| = ||\mathbf{s} - \mathbf{u}|| \tag{2.3}$$

The distance r, is determined by measuring the propagation time of a signal from the satellite to the receiver. If the true time is dt when the signal is sent from the satellite and the true time is dT when the signal reaches the receiver, the geometric distance r can be written as

$$r = c\,(dT - dt) \tag{2.5}$$

where c is the speed of light.

2.1.8.2 Carrier Phase Measurement:

Ideally, the carrier phase measurement would be the number of full and fractional cycles between the satellite and receiver antennas. However, a GPS receiver cannot distinguish one cycle from another, so it measures the fractional phase and keeps track of the changes in the phase. The problem is that it is only possible to measure the phase of the last fraction of a wavelength and not the real distance. There will be an unknown number of whole wavelengths N that cannot be measured directly. The unknown number of wavelengths N is called the Integer ambiguity. Without determining the integer ambiguity, the phase measurement is rather worthless until integer ambiguity is resolved. There are many methods available to resolve the integer ambiguity and have been documented in various research papers. For this reason the carrier phase measurement is ambiguous, and cannot be used alone for GPS positioning [7].

The carrier phase measurement equation is:

$$\Phi = r + r_d + c\,(d_t - d_T) + \lambda N\text{-}ion_d + trop_d + \Phi\varepsilon \tag{2.6}$$

Where:

Φ	observed integrated carrier phase (degree),
λ	wavelength in (m),
N	integer ambiguity (cycles), and
$\Phi\varepsilon$	receiver carrier phase noise plus multipath (degree).

This equation (2.6) is similar to the pseudorange equation, although there are some differences. The most notable difference is the integer ambiguity in the phase measurement equation. The integer ambiguity is the difference in the number of wavelengths between the start of the receiver generated carrier phase and the signal from the satellite. While the magnitude of the ionospheric error is the same on both the code and phase measurements, it has an opposite sign. The ionosphere, delays the code measurement, so the measured range is longer than the true value. In the case of the carrier phase, the signal is advanced by the ionosphere as it propagates through the atmosphere, so the measured range is shorter than the correct value.

2.1.8.3 Doppler Frequency Measurement:

The Doppler measurement is a measure of the difference in velocity between the satellite and antenna, and is typically measured in L1 cycles per second. The Doppler measurement does not have an integer ambiguity, and is in the range of ± 5 KHz. The Doppler measurement is used in calculating the velocity. The equation of the Doppler is:

$$\Phi' = r' + r'_d + c\,(d'_t - d'_T) - ion'_d + trop'_d + \varepsilon'_\Phi \qquad (2.7)$$

Where the dash represents the derivatives with respect to time.

The accuracy of the instantaneous Doppler measurement depends on the receiver architecture and tracking bandwidth of the code tracking loop. Modern GPS receivers can measure the instantaneous Doppler frequency shift with an accuracy of 5 mm/second [8].

CHAPTER 3 GPS ERRORS SOURCES AND THEIR EFFECT

There are a number of possible sources of errors which can degrade the accuracy of positions computed and hence impact the performance of a GPS receiver. These error sources can be mainly categorized into two groups, system wide errors and specific operating environment or specific GPS receiver errors.

3.1 System Wide Sources of Errors

GPS error sources which are systematic in nature and which can be reduced partially or wholly eliminated by means of differential correction technique are summarized in the following figure.

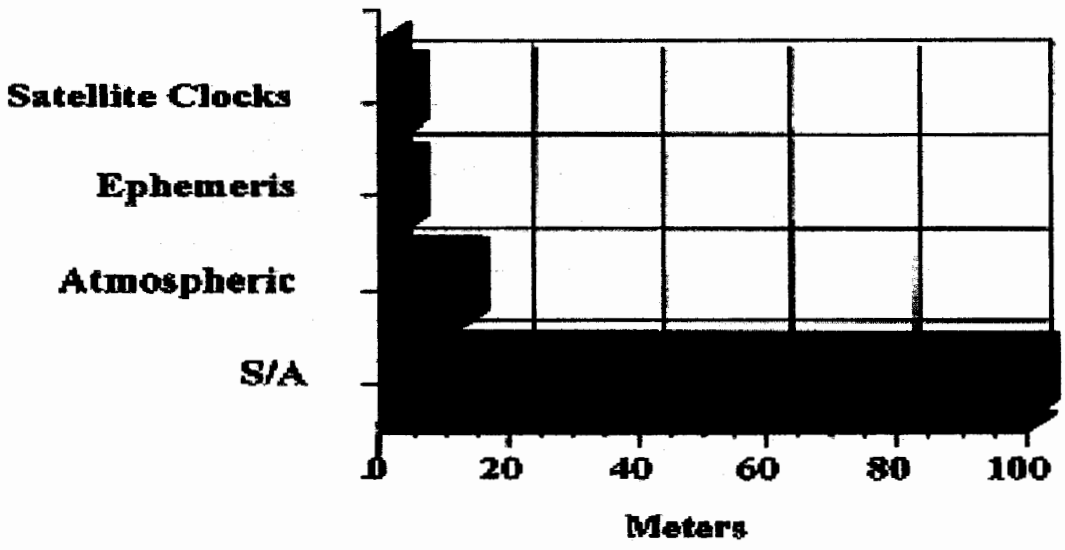

Figure 3.1 System wide Errors and their impact

As can be seen from the above figure the major error is selective availability (S/A), which is an intentional clock error introduced in the satellites by the US Department of Defense to avoid unauthorized people to obtain (in their opinion) a too accurate position. But this error is no longer an issue because in May 2000 the U.S Government removed it. However there is no guarantee from the USA that it will not be introduced again. The typical systematic errors that affect a pseudorange measurement are further classified into the following subclasses:-

1.	Ephemeris data	Errors in the transmitted location of the satellite
2.	Satellite clock	Errors in the transmitted clock
3.	Ionosphere	Errors in the corrections of pseudo range caused by ionospheric effects
4.	Troposphere	Errors in the corrections of pseudo range caused by tropospheric effects

Table 3.1 GPS Ranging Errors

These errors are briefly discussed in the following paragraphs one by one: -

3.1.1 Ephemeris/Orbital Error

Ephemeris errors result due to the inaccuracies in the satellites position reported by the GPS ephemeris message. That is orbital information about satellites as given by the ephemeris data does not match with actual satellite position in real time. The inability to completely model the forces acting on a satellite, and the degradation due to Selective Availability (SA) are the main reasons of orbital errors. Although the satellites are positioned in very precise orbits, slight shifts of the orbits are possible due to gravitation

forces and solar winds. These forces buffet the satellite, causing the true trajectory to differ from the planned one. These forces cannot be estimated and therefore cause an error in the calculation of satellite position from the ephemeris data. If the error is left uncorrected it will result in inaccurate range determination and hence the location of the user position.

Differencing observations between receivers from the same satellite can reduce the error. This method is called DGPS (Differential Global Positioning System) method. In this method two receivers are taken one is called reference or base station and the other one is called rover station. The base station is at known position. Rover station observations are subtracted from the base station and the difference computed is considered as error. Another very effective way to handle orbital errors is to use post-processed precise orbits. Precise orbits are derived from an extensive reference network such as the Cooperative International GPS Network (CIGNET) resulting in the accuracy as high as a few centimetres. The orbit data are controlled and corrected by the ground control stations regularly and this corrected data is sent back to the receivers therefore the ephemeris errors do not have a significant impact on the pseudorange measurements and receiver tracking performance relative to other errors. Tests have shown that the orbital error is generally a few metres.

3.1.2 Satellite Clock Errors

Each satellite carries atomic (rubidium or cesium) clocks which are used as the time and frequency base for the realization of the GPS system time. Although the satellite clocks are very accurate and stable, they are not perfect and there is still chance of errors.

Moreover, the ground control stations of GPS are constantly monitoring the behavior of satellite clock deviations and uploading correction parameters. These parameters are then transmitted to the GPS receivers via the satellite broadcast data, and the receivers can use this information to compensate for satellite clock errors [9].

Differencing observations as explained earlier in section 3.1.1 from the same satellite between two GPS receivers can reduce or eliminate the satellite clock error. An alternative method is to leave the satellite clock offsets as an unknown which is to be determined from parameter estimation at later stage [10]. The following equation can be used for determining the satellite clock error from the ephemeris message.

$$dt = af_2(t - t_{oe})^2 + af_1(t - t_{oe}) + af_0 + d_{rel} - t_{gd} \tag{3.1}$$

where

dt	satellite clock error (s),
af_2	second order coefficient (s^{-1}),
t	time of measurement (s),
t_{oe}	time of ephemeris (s),
af_1	first order coefficient (unitless),
af_0	zero order coefficient (s),
d_{rel}	relativity correction (s), and
t_{gd}	group delay (s)

3.1.3 Atmospheric Errors

The atmosphere affects the GPS signals up to a significant level. As a result the electromagnetic waves are both delayed and refracted because the refractive index of atmosphere's constituent gases is slightly greater than unity. It is known that while passing through the ionosphere the electromagnetic waves are slowed down inversely proportional to the square of their frequency ($1/f^2$). That is electromagnetic waves having lower frequencies are slowed down more as compared to electromagnetic waves with higher frequencies. The resultant decrease in velocity increases the time taken for the signal to reach the receiver antenna, thereby increasing the equivalent path length. At low elevation angles refraction bends the ray-path and further increases the delay. The atmosphere has two critical regions (ionosphere and troposphere) which induce errors in the GPS signal. The troposphere also called the lower part of atmosphere ranges from sea-level to 50km while the ionosphere ranges from 50 to 1500km in the space [11]. The effect of both these regions is discussed in detail in the following subsections.

3.1.3.1 Ionospheric Errors

The ionosphere is a region of the atmosphere which starts at an altitude of 60 to 1500 km. It contains a significant number of free electrons (negative charge) and positively charged ions [12]. The electrons and ions can be divided into four layers in the ionosphere namely D-, E-, F1-, and F2-layer. These layers of free electrons retard the propagation of GPS signals in free space by more than 300 ns in the worst case, resulting in range errors of 100 meters [13]. The density of free electrons also called Total Electron Content (TEC) depends primarily on ultraviolet light rays from the sun; consequently

amount of ultraviolet light determines the state of the ionosphere. In the absence of ultraviolet light, the free electrons and positive ions recombine, which reduces free electrons density. So the free electron density is a function of the relative position of the sun, which makes it vary in a 24-hour cycle when observed from earth.

The total electron content (TEC) along the path from the GPS satellite to the receiver can be defined as:

$$\mathrm{TEC} = \int_{path} N_e \, ds, \tag{3.2}$$

where

Ne is the local electron density, expressed in electrons/m^3.

The ionosphere error can affect both code and carrier phase measurements, as well as increases the probability of losing lock on the satellite. The ionospheric error also depends on the elevation angle, magnetic activity. A typical ionospheric error ranges 5-30 meters. The equation for the phase measurement advance due to ionospheric effect is [6]:

$$d_{ion} = \frac{f_2^2}{f_1^2 - f_2^2}\left(\Phi_1\lambda_1 - \Phi_2\lambda_2 - \left(N_1\lambda_1 - N_2\lambda_2\right)\right) \tag{3.3}$$

where:

f_1, f_2 frequency of band L1 or L2 (Hz) respectively,

λ_1, λ_2 wavelength of L1 or L2 (m) respectively,

Φ_1, Φ_2 carrier phase measurement on L1 or L2 (cycles) respectively, and

N_1, N_2 integer ambiguity on L1 or L2 (cycles) respectively.

3.1.3.2 Troposphere Errors

Troposphere is the lowest part of atmosphere and ranges up to 16 km in altitude from the surface of the earth although the neutral atmosphere extends up to 60 km. The main factors which cause troposphere delay include temperature, pressure and humidity. The delay also changes with the height of the user position and the type of terrain below the signal path can change the delay. According to Hopfield [14], there are two component of troposphere delay namely wet delay and dry delay. The dry component which causes delay up to 80-90% of the total delay is easier to be determined as compared to the wet component. The following table shows in average numerically both components of the troposphere delay under different elevation angle.

TH 7402

1.	90°	2.3	0.2	2.5
2.	20°	6.7	0.6	7.3
3.	15°	8.8	0.8	9.6
4.	10°	12.9	1.1	14.0
5.	5°	23.6	2.2	25.8

Table 3.2 Tropospheric Delay on Measured Range

The dry delay is mainly caused by the O_2 and N_2 gases present in the atmosphere and it can be modeled up to 1% or better. On the other hand the wet delay which causes up to 10-20% of the total delay is difficult to modal. The wet delay is due to the presence of water vapors in the atmosphere.

Mathematically the tropospheric delay T can be represented as

$$T = \int_{path} (n \quad 1) ds + \Delta_g \tag{3.4}$$

where

n is the refractive index of the atmospheric gases and

Δ_g is the difference between the curved and free-space paths.

A number of models have been developed by different researchers to estimate the tropospheric delay. Some of the popular models are, the Hopfield model (Hopfield, 1969), the modified Hopfield model (Goad and Goodman, 1974), and the Saastamoinen model (Saastamoinen, 1973). However the error introduced by the troposphere is impossible to predict in real time, being affected by the weather conditions between the receiver and satellite (the amount of water in the line of sight to the satellite being the major factor).

The troposphere delay is a non-dispersive in nature that is the delay effects are not frequency dependent. It means the delay is same for both the code and phase measurements. Without appropriate compensation, tropospheric delay will induce pseudorange and carrier-phase errors from about 2 metres for a satellite at zenith to more than 25 metres for a low elevation satellite. The effect is to both retard the velocity of the signal and to refract (bend) its ray path.

3.2 Local GPS Error Sources

There are some GPS error sources which are local to a specific operating environment, or specific to a particular GPS receiver design. Such errors can be further classified in to two sub class's namely environmental error and receiver related errors. Environmental error sources include: multipath and geometry of satellite while GPS receiver related factor are receiver channel noise and clock error.

It should be kept in mind that local error sources cannot be eliminated by the differential correction approach. The only way to resolve the errors is to use good GPS receiver technology and operate in suitable environment, in order to minimize environmental error factors. Recent improvements in GPS receiver design has increased the resistance to multipath and RF interference, but have not eliminated these factors completely.

1.	Multipath	Errors caused by reflected signals entering the receiver antenna.
2.	Satellite Geometry	Errors due to the shape of the satellite visible to user.
3.	Receiver Noise	Errors in the receiver's measurement of range caused by thermal noise, software accuracy and interchannel bias.
4.	Receiver Clock	Errors in the receiving clock.

Table 3.3 Local GPS Error Sources

In the following paragraphs each of the above error is described briefly.

3.2.1 Multipath Errors

Generally the term multipath can be defined as when replicas of a radio signal arrives at the receiver antenna through more than one path with different delay of time such phenomenon is known as multipath. In the case of GPS this phenomena also occurs and introduces error in the GPS signal and ultimately in the user position measurement. Multipath error is caused by surroundings building, hills, trees and other obstacles lays in the way of the GPS signal. As a result, it is highly dependent upon the conditions surrounding the receiver antenna, the type of antenna that is used, and the signal tracking algorithms of the receiver [15]. The multipath effect can be depicted as shown in the following figure.

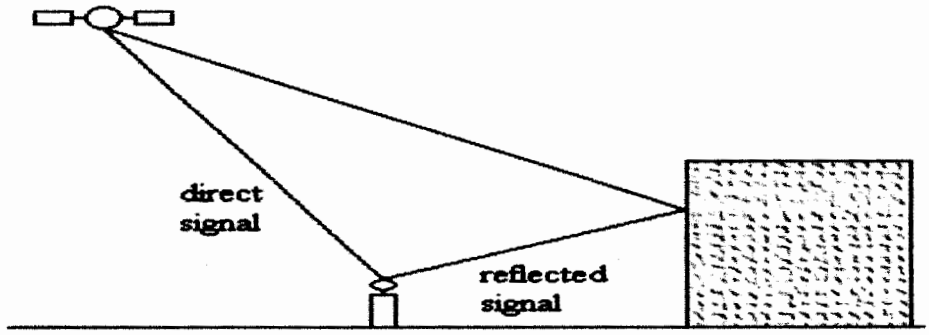

Figure 3.2 Multipath Effect

The common numerical value of error introduced by multipath effect is 3 m for code measurement and 0.5 cm for phase measurement. Multipath error can be reduces up to greater extent by selecting suitable observation site, special type of antenna and advanced receiver having suitable tracking algorithms such as narrow correlator spacing, Multipath Elimination Technology (MET) and Multipath Estimating Delay Lock Loops (MEDLL). Result had shown that MEDLL was the most effective method at reducing multipath error compared to the other methods as described earlier [16].

Antenna based multipath mitigation involves improving the antenna gain pattern to counter the multipath. A choke ring with a ground plane has shown best result in this regard. Significant improvements can be achieved by developing an antenna with a very low gain for left hand circularly polarized (LHCP) signals and using an antenna array to have a sharp cutoff below a certain elevation angle.

3.2.2 Satellite Geometry

The geometric constellation or shape of satellites visible to a GPS user can also impact the accuracy of position determined by a receiver. This effect is known as Dilution of Precision (DOP). DOP can be explained better with following diagram.

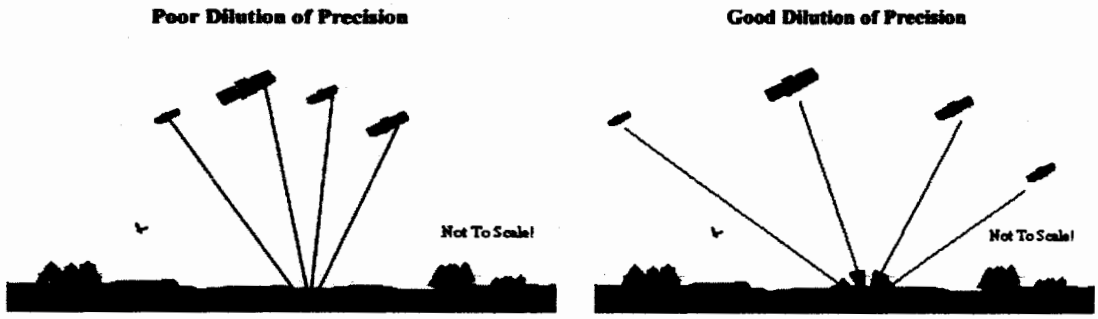

Figure 3.3 Comparison of High and Small DOP

Mathematically the relationship between the position of the satellites and range measurement can be expressed as follow [17]:

$$\sigma_p = DOP * \sigma_r \tag{3.5}$$

where:

σ_p	standard deviation of point position (m),
DOP	dilution of precision (DOP), (unitless), and
σ_r	standard deviation of range measurement (m).

The DOP can also increase or decrease other types of GPS errors. It means better the geometry of the satellites lesser will be the chance of error. It usually depends on the angle among the satellites i-e greater the angle among the satellites more accurate will be the position calculation. There are different variants of DOP such as HDOP (Horizontal Dilution of Precision), VDOP (Vertical Dilution of Precision), TDOP (Time Dilution of Precision) etc. All of these variants values are summed together to give a common value for GDOP (Geometric Dilution of Precision). The average error value caused by the satellite geometry is 2.4 m which can reach up to 10 m or more in case of poor satellite geometry. DOP with greater value represent poor geometry and vice versa.

3.2.3 Receiver Noise

Errors which result due to the internally operated measurement procedures used within the receiver are typically grouped together as receiver noise. The receiver noise is considered as white noise in GPS receiver for specific time period. As the tracking loops incorporated in both GPS Carrier phase and code measurement are not same therefore it is generally believed that the noise is uncorrelated. The tracking loop jitter is the main reason of the noise [15]. It was also shown by Raquet that the noise level can be decreased to a greater extent by taking the GPS data on high elevation angle. The angle

can be increased up to about 45°, where the noise becomes constant. The code measurement noise level decreases from 58 cm to 15 cm as the elevation angle increases.

Modern receiver technology have shown best result and decreased phase noise level up to 1 mm, and on the other hand reduced the code noise to the ten centimeter level.

3.2.4 Receiver Clock Error

Receiver clock error is the difference between the receiver clock and the GPS system time. The magnitude of the error depends on the receiver's internal structure like the type of oscillator used in the receiver. The receiver clock error leads to a range error in the pseudorange and carrier phase measurements. Similar to the satellite clock error, the receiver clock error can be eliminated or reduced to greater extent by differencing between the observations observed in a receiver between two different satellites.

Besides these there are some other errors like relativistic effect, rounding off error and measurement which can lead from 1 m to 2 m error. In short the errors of the GPS system are summarized in the following table. The individual values are no constant values, but are subject to variances. All numbers are approximate values.

1.	Ionospheric effects	± 25 meters
2.	Troposphere	± 25 meters
3.	Shifts in the satellite orbits	± 2.5 meters
4.	Clock Drift both satellite & Receiver	±1.5 meters
5.	Multipath	±1 meters
6.	Selective Availability	±70 meters
7.	Receiver Noise	±10 meters
8.	Calculation- and rounding errors	±1 meters

Table 3.4 GPS Errors

CHAPTER 4 LITERATURE REVIEW

The sources of errors in GPS navigation (satellite clock, receiver clock, atmospheric and multipath errors) induce biases in the measurement of pseudo range and degrade system accuracy in case of commercial GPS receivers employing the C/A code.

In recent years, many researchers have studied and documented GPS errors. Some of these researchers have also analyzed the effect of errors on GPS positioning.

4.1 Errors Sources

In the last several decades, numbers of models have been developed and reported in the scientific literature by researchers for estimating the delay induced by the troposphere in the GPS signal. However, much research has gone into the creation and testing of tropospheric refraction models to compute the refractivity N along the path of signal travel. These models includes Hopfield, 1969; Saastamonien, 1973; Goad and Goodman, 1974; Santerre, 1987; Marini, 1972; Baby et al., 1988; Mendes and Langley, 1994 and Edward E. Altshular et.al 1998. All these models work fairly well, but they do generally require input of meteorological parameters which may have errors. Also, the troposphere is at times not homogeneous (such as when a storm front is moving through), which can result in errors. Some of these models will be discussed briefly below.

Hopfield [18] developed a dual quartic zenith model of the refractivity with different and separate quartics for the dry and wet atmospheric profiles. He described that refractivity is function of height above the surface assuming single polytropic layer. The model given by Hopfield has been simplified and modified later on by many scientists over the years such as Goad and Goodman (1974), Black (1978), Kouba (1979) etc.

Saastamonien [19] described a standard model for RF tropospheric delay valid for $\varepsilon \geq 10^{\circ}$ elevations and then Saastamonien refined his model by adding two

correction terms, one dependent on the height of the observation site and the other on the height and the zenith distance.

Edward E. Altshular et.al [20] presented an algorithm for estimating the tropospheric range error from the user height above sea level, latitude, day of year, and elevation angle to the satellite from the GPS receiver. He has demonstrated in his paper that range error produced by troposphere is approximately 25 m for an elevation angle of 5°.

Theodore L. Beach, Paul M. Kintner, et.al [21] has developed a specialized ionospheric scintillation monitor also called the Cornell scintillation monitor which monitors L-band amplitude scintillation. They have demonstrated the successful modification of a commercial GPS receiver development system to monitor variations in signal strength at a rate of 50 samples/s. They also argue that the Cornell scintillation monitor can record scintillations from several GPS lines of sight simultaneously and permits correlation studies with multiple receivers. Additionally, observations of signal strength fluctuations from day to day may provide insight into the multipath environment of a stationary antenna installation. According to them the results obtained from these investigations are being used to better characterize equatorial L-band scintillations and their potential effects on the operation of GPS receivers.

Siti Sarah Nik Zulkifli, Mardina Abdullah, et.al [22] studied the ionospheric error on transionospheric signal propagation from satellite to ground paths using readily available GPS satellites utilizing Jones 3-D ray-tracing algorithm. They measured the value of absolute range error (group delay) and relative range error (phase advance) when a signal propagates in the ionosphere. The ionospheric delay or advance is obtained from the difference between the distance of the ray path to the receiver from the satellite determined from the ray-tracing and the distance for propagation over the LOS at the velocity of light in vacuum. The value of RRE is then calculated. RRE is the difference between the standard dual frequency models corrected range and LOS. Results show that the RRE of group value is different from the RRE of phase advance.

Other researchers like Goad, Cohen et al. and Hansen et al. have also devised methods to estimate ionospheric delays.

Multipath effects on pseudorange measurements have been studied for almost two decades. Hagerman [23] derived relationships involving multipath and code-tracking error. This fundamental work formed the basis for the analysis of GPS code and carrier multipath.

Evans [24] demonstrated multipath effects on ionospherically corrected code and carrier phase measurements from geodetic receivers. Georgiadou and Kleusberg [25] considered multiple reflections and showed that multipath on short baselines could be detected using dual frequency measurements. Abidin [26] examined the effects of multipath on ambiguity resolution for dual frequency measurements.

4.2 Mitigation Techniques

While some researchers have documented the effect of errors on GPS accuracy, others have developed algorithms and techniques to mitigate these errors in order to improve GPS position fix. Few of them are briefly outlined in the next paragraphs.

Tajul A. Musa, et.al [27] in his study proposed geometric modeling through the network-based approach to mitigate the residual tropospheric delay in low latitude area of troposphere region. They performed tests in post-processing but in the "simulating RTK" mode, and evaluated the number of ambiguity fixes and the accuracy of the coordinate results. According to them network based RTK positioning in low latitude areas has shown that the proposed technique can enhance ambiguity resolution by pivoting the ionosphere-free measurements through the mitigated residual tropospheric delay.

JiHong Zhang [28] proposed a method named Trop_NetAdjust which not only predicts the residual tropospheric delays on the GPS (Global Positioning System) carrier phase observables using redundant measurements from a network of GPS reference stations but also enhances the effectiveness and reliability of the integer ambiguity

resolution process. Besides this the technique can be a good approach for tropospheric parameter variation forecasting.

Hopfield in [29] discussed two types of improvements in tropospheric range correction which are based on a model developed by the same author earlier. One of the two improvements described by him is correction for signal path bending, and the other is an improvement of the model N profile shape. The author recommends that signal path bending correction should be made prior to the profile shape correction.

An algorithm was designed by John A. Klobuchar [13], which uses eight coefficients, transmitted as part of the satellite message, to provide a correction for approximately 50 percent rms of the ionospheric range error. Further the author described that corrections for ionospheric range rate errors for a single frequency user are not practical by modeling techniques, due to the impossibility of predicting, except in a statistical manner, the small undulations in the ionosphere which produce range rate errors on time scales of a few seconds to minutes. The goal of a 50 percent rms correction for the ionospheric algorithm was arrived at somewhat arbitrarily as a compromise between number of coefficients required to be sent as part of the satellite message and the realization that even a state of the art ionospheric model, requiring many coefficients, would provide only a 70 to 80 percent rms correction to the ionospheric time delay.

A simple formula has been derived by M. Mainul Hoque, et.al [30] to mitigate higher order ionospheric error. According to the author, the proposed correction algorithm reduces the second order effects to a residual error of fractions of one millimeter up to two millimeter at a vertical TEC (Total Electron Content) level of 1018 electrons/m2 (100 TECU), based on satellite azimuth and elevation angles. The correction formula can be used in real-time applications as it does not needs the information of the geomagnetic field or the electron density distribution in the ionosphere along the signal path. It is expected that the correction will enable more accurate positioning using the line-of-sight carrier-phase measurements.

S. Choy, et.al [31] evaluates the performance of three different ionospheric error mitigation methods in terms of the accuracy and precision of the derived solutions, as well as the time required for the solutions to converge. The tested mitigation algorithms are used in single frequency PPP (Precise Point Positioning), known as GRAPHIC (GRoup And PHase Ionospheric Correction) algorithm developed originally by Yunck, in 1993, the Global Ionospheric Maps (GIMs) developed by IGS and the Klobuchar model. Based on the numerical results derived, the author shows that the GRAPHIC and GIMs methods are able to provide point positioning accuracy better than one meter for session duration less than an hour using geodetic quality single frequency receivers. For 12 to 24 hours data sets, the positioning accuracy can be as good as <0.1m.

J.K.Ray, M.E.Cannon [32], investigated the effect of carrier phase multipath in static mode and developed a system to reduce the effect using multiple closely-spaced antennas. According to them correlated nature of multipath, along with the known geometry among the antennas, are used with the measured relative carrier phase differences to aid in the extraction of the direct carrier phase from the multipath-corrupted carrier phase measurement. They also presented mathematical model of the multipath effects on carrier phase measurements and implemented the Kalman filter to estimate these errors.

The above mentioned technique estimates the parameters of the composite multipath signal and removes the error due to all multipath signals. It is particularly useful in case of reference stations which transmit carrier phase data for kinematic positioning applications.

An adaptive filter technique based on a least-mean-square (LMS) algorithm was developed and used by Linlin Ge, et.al [33] to mitigate the multipath errors. Furthermore as argued in [34], this algorithm is suitable for real time applications.

Numerical simulation studies indicate that the adaptive filter is a powerful signal decomposer, which can significantly mitigate multipath effects. By applying the filter to

both pseudorange and carrier phase multipath sequences derived from some experimental GPS data, multipath models have been reliably derived. It is found that the best multipath mitigation strategy is forward filtering using data on two adjacent days, which reduces the standard deviations of the pseudorange multipath time series to about one fourth its magnitude before correction and to about half in the case of carrier phase. The filter has been successfully applied to the pseudorange multipath sequences derived from CGPS data. The benefit of this technique is that the affected observable sequences can be corrected, and then these corrected observables can be used to improve the quality of the GPS coordinate results.

Calmin D. Scarlett [34] showed that cellular based GPS error correction system can be implemented. He also argued that the system is geared towards reducing and/or eliminating these errors and thus increasing the accuracy of the GPS system. This system is able to provide the same services as the Differential GPS (DGPS) systems which are in use today.

David Hadaller [35] proposes simple software techniques to mitigate systematic errors caused by mobility in off-the-shelf devices. Similarly ANN (Aritificial Neural Network) technique was used to reduce the position errors as discussed by Sarawut Nontasud et al, [36].

Colombo [37] studied precise GPS positioning over long baselines using a software simulation (Colombo, 1991). A high-order Kalman filter/smoother was used to estimate satellite position errors, reference receiver position errors, atmospheric refraction errors, mobile receiver position, and phase ambiguities using dual frequency carrier-phase and single frequency L1 Coarse Acquisition (CA) code measurements. There were no multipath errors in this simulation. He showed that using the high-order model (versus estimating only position and velocity) significantly improved positioning accuracy, especially when there were large satellite orbit errors. He also showed that using two reference receivers improved the results. However, the smoothing portion of this near-optimal method can only be performed in post-mission mode.

Besides the techniques discussed above to mitigate the errors introduced by the different GPS error sources another popular technique known as DGPS (Differential Global Positioning System) can be used to alleviate errors such as satellite and receiver clock errors and ephemeris error to improve the GPS position accuracy.

Ehsani et al. [38] explored how less than three meters of accuracy can be achieved using differential techniques that use additional signals sent from known ground stations.

Centimeter level positioning accuracy can be achieved using carrier phase-based Differential GPS (DGPS) technique, in which two or more geodetic quality GPS receivers are deployed and two or more frequencies are used to alleviate ionospheric effects ,Wang et al., 2004 [39], Wu et al., 2006 [40]. This technique is able to provide high accuracy solution because common errors, such as satellite and receiver clock errors are cancelled out in short baselines or the errors are dramatically reduced in long baselines, Zhang et al., 2007 [41].

CHAPTER 5 SIMULATION AND COMPARISON OF RESULTS AND ANALYSIS

The simulation work was carried out in the software Matlab version 7.3 on actual GPS data using software GPS receiver. The results of simulation performed have been recorded and important ones are given below.

5.1 Capturing of GPS Data

The GPS data used in this project has been acquired using a National Instruments PCI-6534 DAQ board, installed in a PC. File sizes up to 2×10^9 bytes have been captured in this manner (106 seconds at 19.2 MB/s. The GPS data was captured in Room E44b of Sackville street building of the University of Manchester. A commercial off the shelf helical antenna was used. It was mounted on a mast and pushed out of the room window during measurements to have a good view of the sky. As usually done the GPS signals were received, amplified, down-converted, and digitized into base band samples. The base band samples are then processed using software routines to acquire and track the direct GPS signal and to generate the receiver position information as explained following sections. The numbers of available satellites were limited to five on the particular afternoon, when measurements were performed. They were however enough to perform the tracking and position calculations as mentioned below in the section 5.3.

5.2 Analysis of GPS Data

The analysis of the data started with the generation of two types of plots as shown in the figure 5.1.

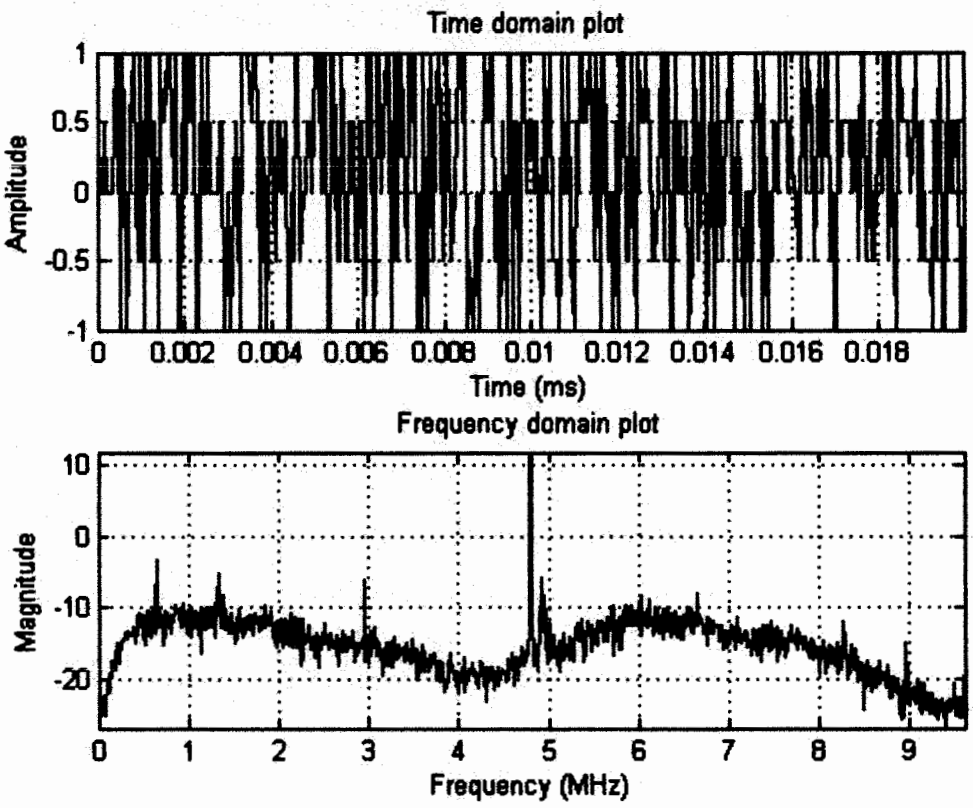

Figure 5.1 Time and Frequency Domain Plots for the Actual GPS Data

The first plot in the figure depicts the time domain plot for 1000 samples. As expected no discernable structure is visible despite the 4.78 MHz IF for the collected data, which is in line with the text explained earlier that GPS data set is a traditional CDMA signal, submersed in white noise and only with the help of correlation theory the data can be demodulated.

5.3 Acquisition and Tracking of Satellites

The first step in the simulation was to acquire satellites from the captured GPS data. The acquisition plot for the captured GPS data is shown in figure 5.2. Only four satellites have strength greater than the acquisition threshold set at 2.5. This is an arbitrary level and can be revised based on the circumstances.

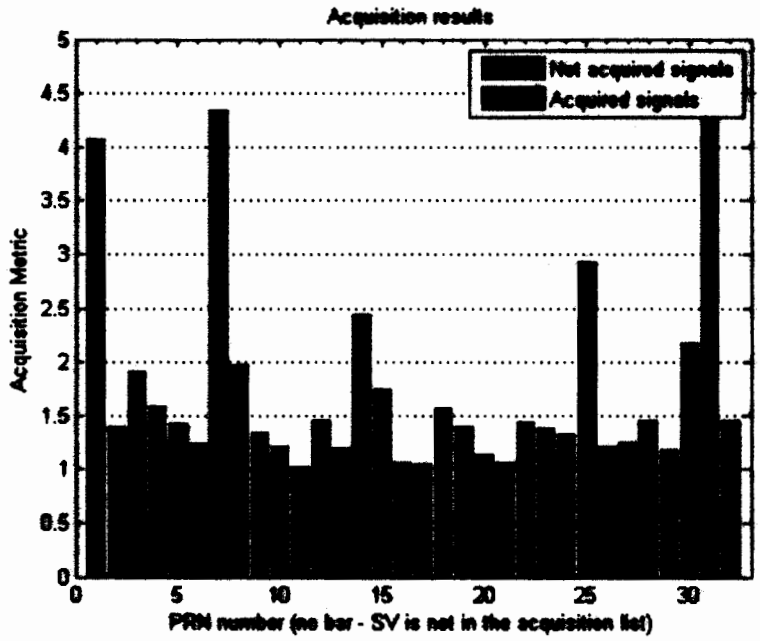

Figure 5.2 Acquisition Results

The purpose of the acquisition process is to identify if a certain satellite is visible or not. If the satellite is visible, the acquisition process determines the coarse values of carrier frequency and code phase of the satellite signals. The list of acquisition specific variable is as follows:

Sr#	Variable	Description
1.	acq_satelliteList	A set of satellites PRNs can be specified, however the default list starts a search for all available satellites (1 to 32)
2.	acq_searchBand	Specifies the frequency band in which to search and is centered around the IF (kHz)
3.	acq_threshold	Determines the threshold of the signal detector

Table 5.1 Description of Acquisition Specific Variable

The parameters i-e carrier frequency and code phase are further refined by the tracking process. That is the main purpose of tracking is to refine the coarse values of code phase and frequency, and keep track of these as the signal properties change over time, thus the tracking code runs continuously to follow the changes in frequency as a function of time.

The plots in the following diagram depict the bits of navigation message and discriminator outputs. As explained in [42] the implemented DLL discriminator is the normalized early minus late power which is filtered to provide feedback in sample precision in order to update the code offsets. For the PLL case arc-tan function is chosen as the phase discriminator and a first order loop filter is employed to predict and estimate any relative motion of the satellite and adjust minor changes to the Doppler frequency. The tracking results for only two of the four channels have been shown due to similarity among diagrams of different channels [3].

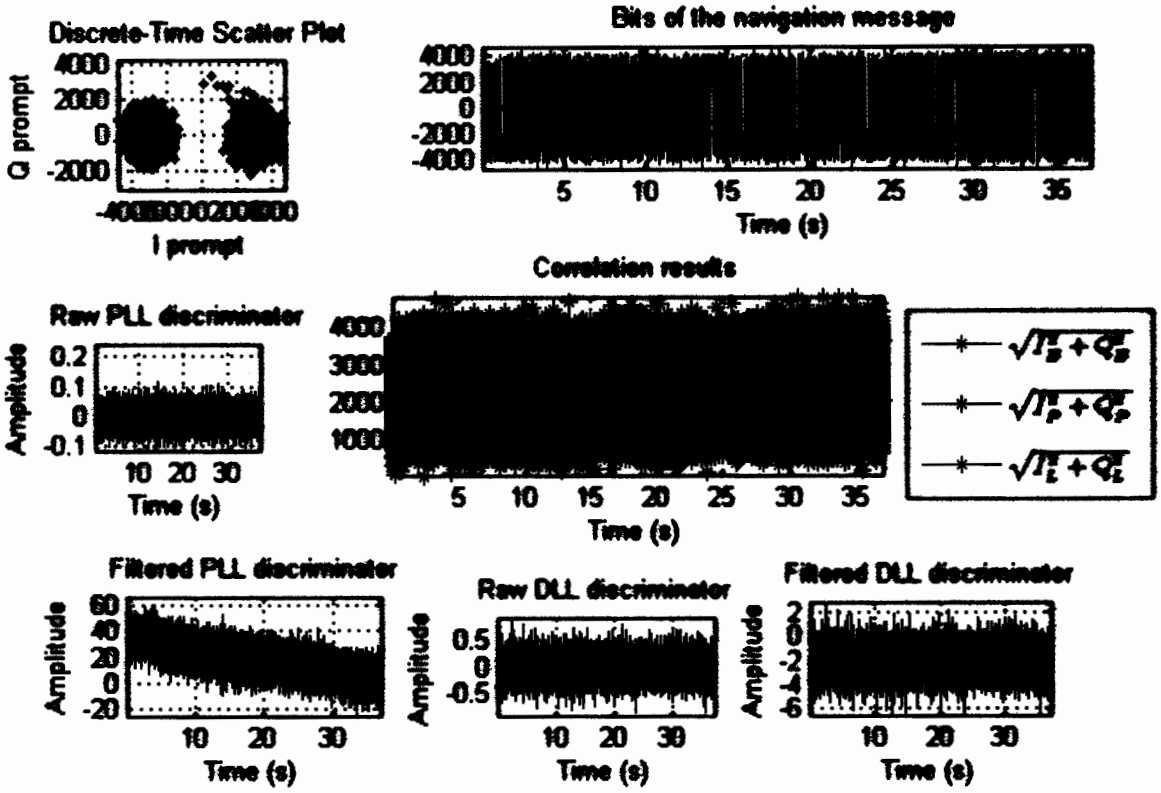

Figure 5.3 Tracking Results for Channel 2

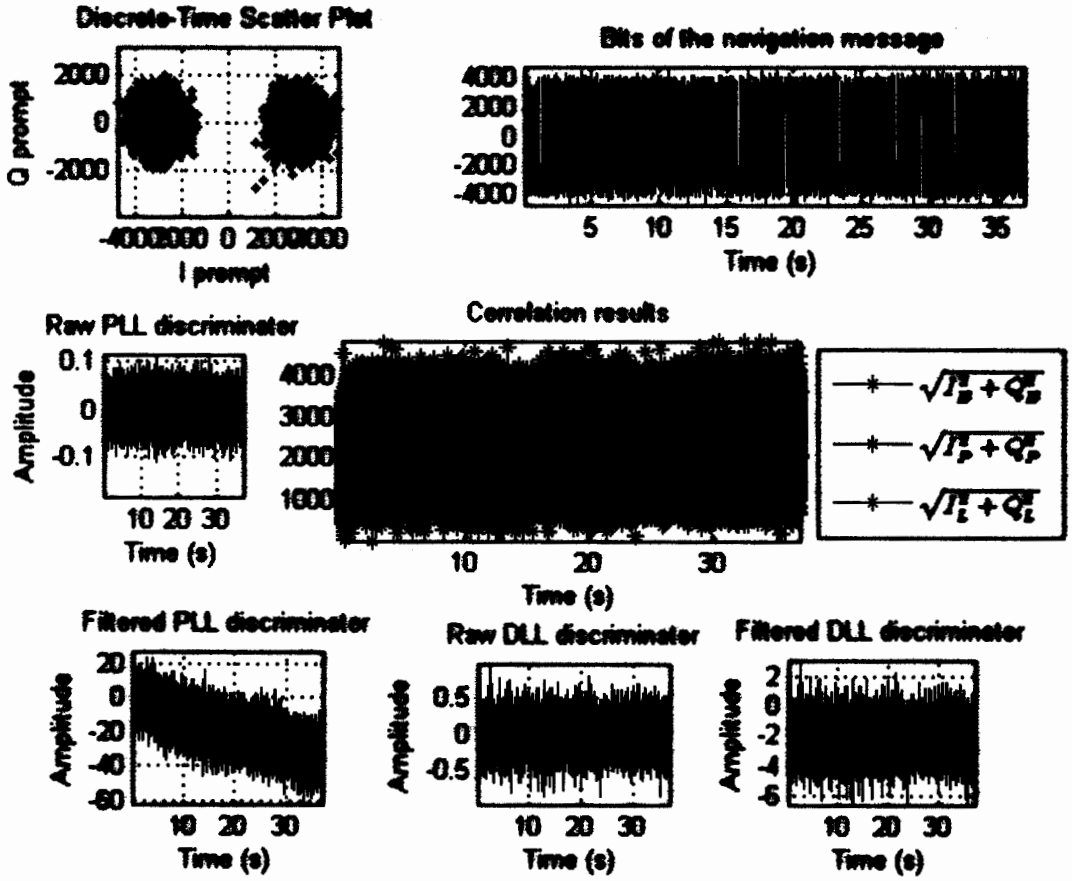

Figure 5.4 Tracking Results for Channel 4

The position calculations were made from 37 seconds of data. This length makes it possible to decode a complete frame of navigation data including all ephemerides for the visible satellites. We know that the geographical coordinates (φ, λ) locate a point on the reference ellipsoid. For many practical purposes it is useful to have coordinate transform in a two dimensional plane. The mapping of an ellipsoid into a plane is performed by conformal mapping. The most commonly used system is the Universal Transverse Mercator Grid System (UTM). In this method the earth is divided into 60 sections that are termed as zones. Each zone covers 6° in longitude and numbered 1 to 60. The coordinates are called northing N and easting E. The transformation of geographical coordinates (φ, λ) into UTM coordinates and vice versa often appears in practical situation. The M-files for this purpose are given in the appendices of [3]. Figure 5.5 plots variations of coordinates over time in UTM system and the mean value in geographical coordinates (φ, λ) depicted in the legend of figures 5.8 and 5.9 is considered as the receiver position. Descriptions of some parameters for carrier tracking are as follows: -

S/N	Variable	Description
1.	PLL_dampingRatio	The damping factor is a well known term in control engineering and controls how fast the filter reaches its settle point and how much overshoot the filter can perform. Hence the choice of damping factor is a compromise between overshoot and settling time. The damping ratio is chosen to be $\zeta = 0.7$ resulting in a filter that converges reasonably fast and does not make a high overshoot.
2.	PLL_noiseBandwidth	The noise bandwidth controls the amount of noise allowed in the filter. A large noise bandwidth helps the tracking loop to lock quickly to the real frequency, but has a relative large frequency noise in the locked state. Similarly a smaller noise bandwidth results in more time before the tracking loop can be locked, but after the lock the frequency is stable. In some software receivers, the PLL is divided into two filters. One filter, having larger noise bandwidth, is used to acquire lock on the signal and other to track the signal in a locked state.
3.	DLL_CACorrelatorSpacing	Spacing between the early and late correlators, usually half chip (unit of chip)
4.	DLL_dampingRatio	Damping ratio for the delay lock loop
5.	DLL_noiseBandwidth	Noise bandwidth for the delay lock loop

Table 5.2 Description of Important Parameters

5.4 Function Tropo

This Matlab subroutine is based on modified Hopfield tropospheric model [45]. The tropospheric correction model used in the simulation was selected because it gives best results as compared to other tropospheric models and it is used widely for tropospheric correction. It calculates tropospheric correction which has to be made to the computed user position. Correction in meters is stored in variable ddr. The range correction ddr in m is to be subtracted from pseudo-ranges and carrier phases.

Descriptions of some important parameters of the Tropospheric correction function are as follows.

S/N	Parameter	Description
1.	sinel	sin of elevation angle of satellite.
2.	hsta	Height of station in km.
3.	p	Atmospheric pressure in mb at height hp.
4.	tkel	Surface temperature in degrees Kelvin at height htkel.
5.	hum	Humidity in % at height hhum.
6.	hp	Height of pressure measurement in km.
7.	htkel	Height of temperature measurement in km.
8.	hhum	Height of humidity measurement in km.

Table 5.3 Description of Important Parameters of Tropo Function

For comparison purposes, positions based on point located approximately at the same location on Garmin Map source were recorded and the result have been compared in table 5.4.

S/N	Description	Latitude (φ)	Longitude (λ)
1	Software results before correction	53° 28' 32.5499''	2° 14' 4.3713''
2	Software results after correction	53° 28' 31.9551''	2° 14' 7.5195''
3	Map results	53° 28' 32''	2° 14' 7.4948''

Table 5.4 Comparison of Results Obtained for Position Calculations before and after tropospheric correction

5.5 Position before and after Tropospheric Correction

Position was computed before and after atmospheric i-e troposphere error correction and effect of the error was noted which can be seen from the figures 5.5 to 5.9. Difference in latitude value was noted and also a significant variation can be seen in coordinates in UTM system from the above figures. Results for 70 ms (millisecond) out of 500 ms (millisecond) data are shown in the following figures.

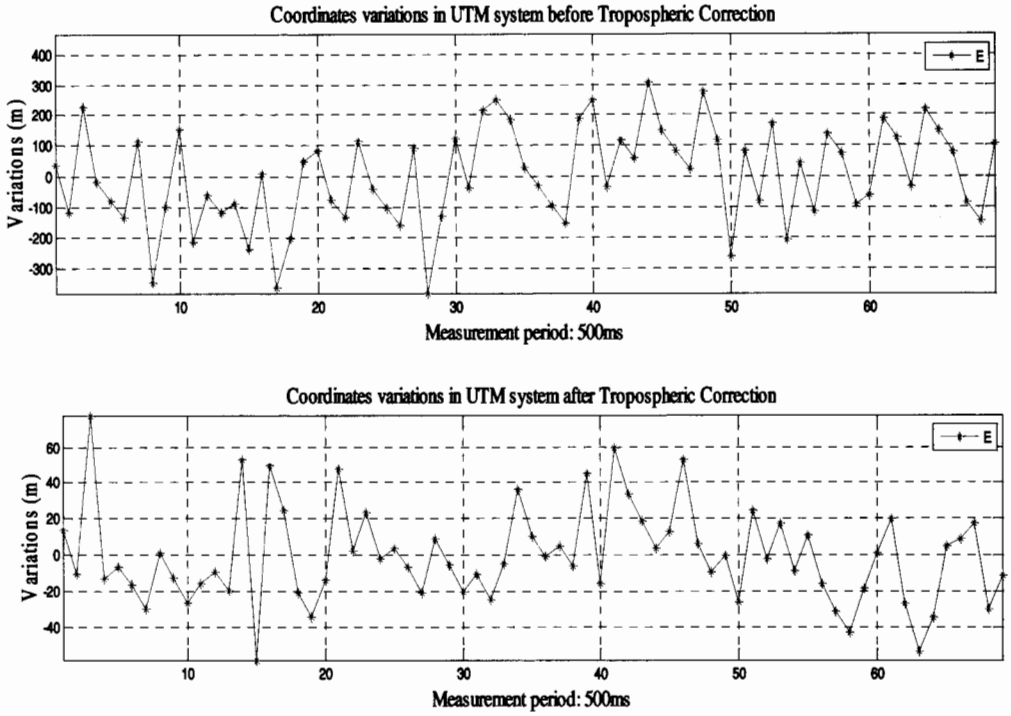

Figure 5.5 East Coordinate variations with and without Tropospheric Correction

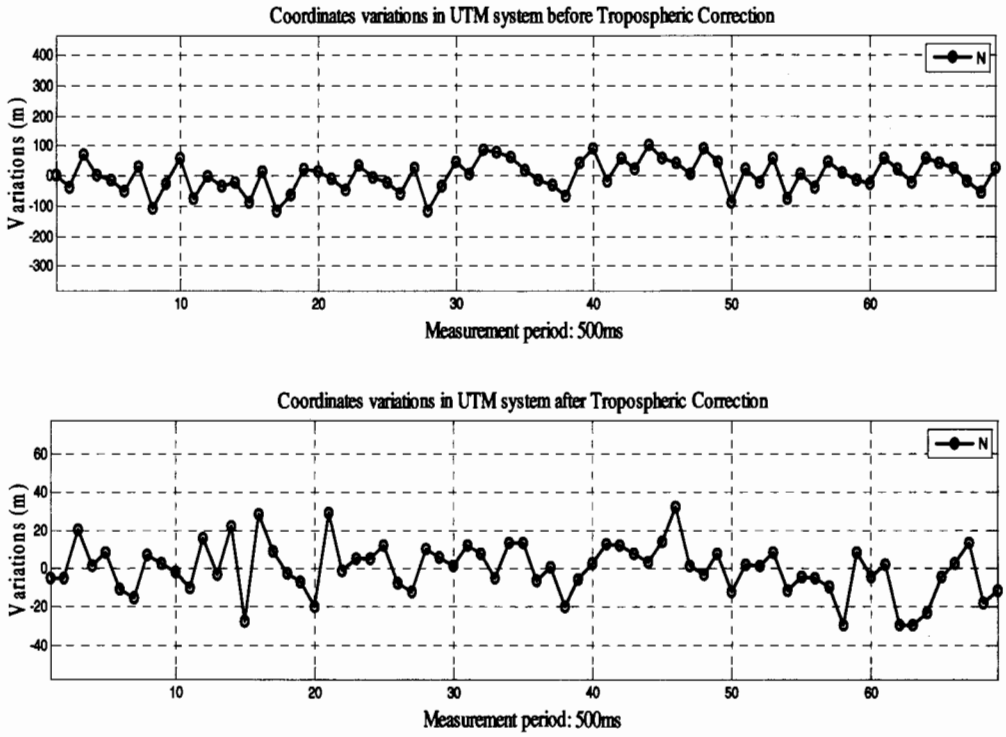

Figure 5.6 North Coordinate variations with and without Tropospheric correction

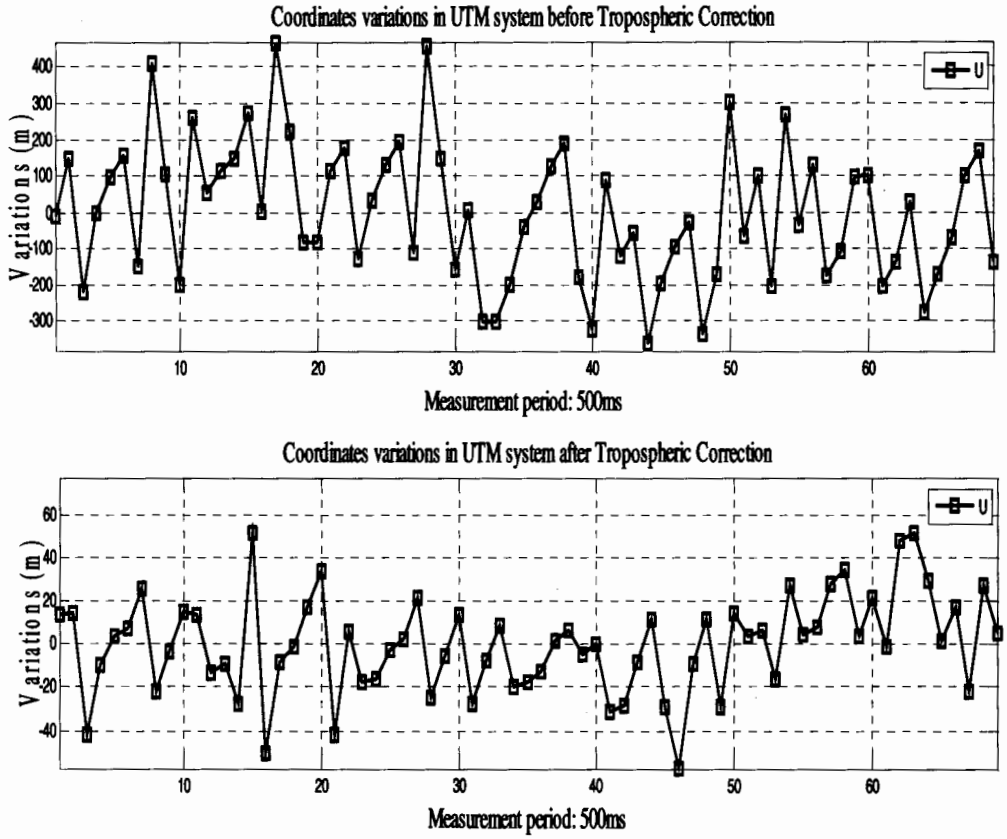

Figure 5.7 Height (Uping) Coordinate variations with and without Tropospheric correction

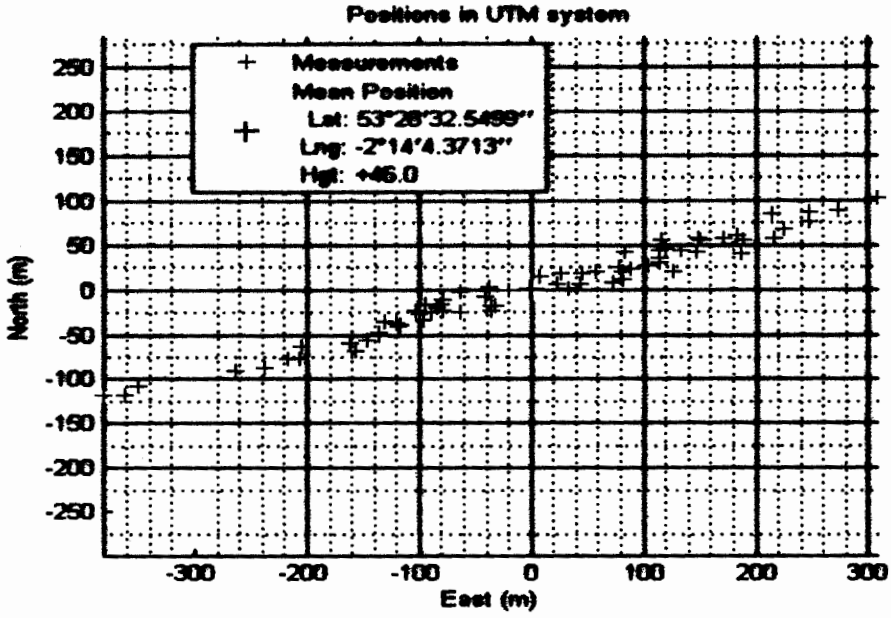

Figure 5.8 Position before Troposphere correction

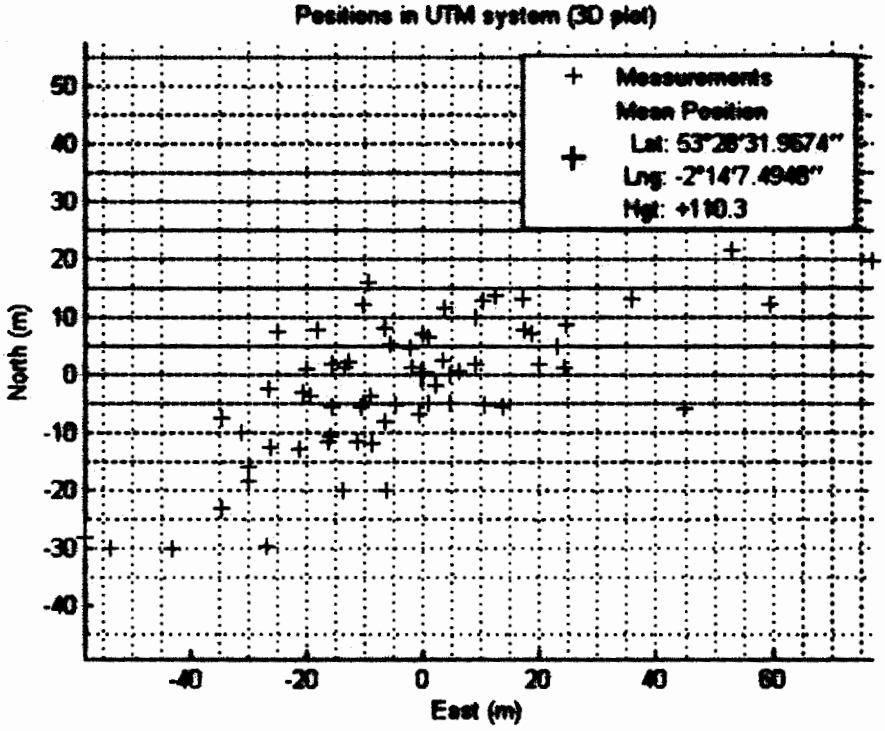

Figure 5.9 Position after Troposphere correction

As can be seen from figure 5.9 the estimator is unbiased because the measurements taken after correction are close to the mean error is zero.

The sky plot in figure 5.10 shows which satellites were visible and tracked when GPS data was captured. The satellites are shown using their PRN number inside the figure. This figure also shows that the value of mean Position Dilution of precision (PDOP) is 7.8783 which is calculated using following equation. High DOP values are found when satellites are clustered together. Practical experience has revealed that it is best to have satellites spaced evenly around the receiver with one satellite overhead and one low on the horizon. Good observations are achieved when PDOP is less than 5 and measurement come from at least five satellites [43]. Mathematically PDOP is calculated as

$$PDOP = \sqrt{\delta_N^2 + \delta_E^2 + \delta_N^2 + \delta_T^2} \quad (1)$$

Where $\delta_N^2, \delta_E^2, \delta_N^2$ *and* δ_T^2 are variances of east, north and up components of receiver position estimate and δ_T^2 is the variance of the receiver clock offset estimate. The relationship between the precision of the pseudorange and the precision of the GPS receiver position calculations is as follows [44].

$$X_{RMS} = \sigma_p x \cdot PDOP \quad (2)$$

where X_{RMS} is the error on the receiver position σ_p is the standard deviation of the pseudorange measurements. So to optimize the accuracy of the position calculation the standard deviation of the pseudorange measurements and PDOP have to be minimized. This may account to small difference in positions calculations.

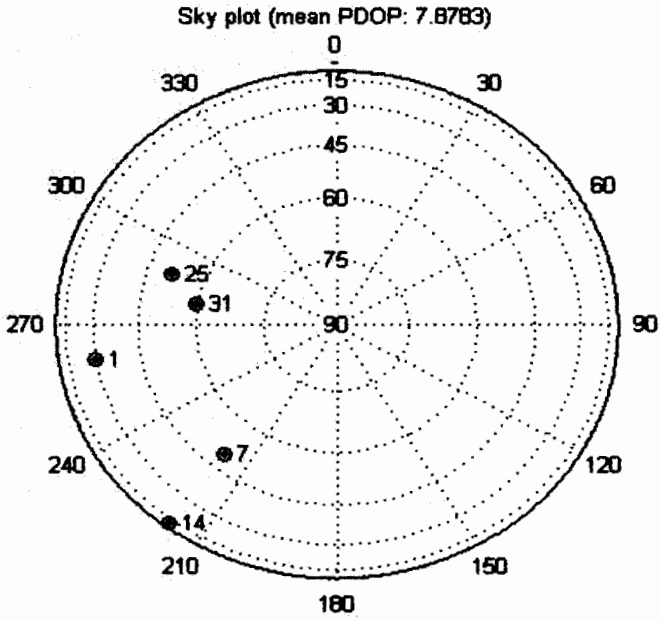

Figure 5.10 Satellite Sky Plot

CHAPTER 6 CONCLUSION AND RECOMMENDATIONS

In the current research endeavor different error sources and their impact on GPS position accuracy was analyzed. Besides this different currently used technique to reduce these errors for improved GPS positioning were also analyzed. Special emphasis was focused on atmospheric errors. In this regard a tropospheric error correction model was simulated on real captured GPS data and results were analyzed.

In future instead of performing absolute positioning of the receivers, relative positioning between receivers will be performed, so that the correlated portion (atmospheric and satellite position) of the measurement errors can be reduced, which will result in a significant increase in position accuracy.

To achieve the desired accuracy two or more GPS receivers will be installed on the system (airborne platform or ground vehicle) and the output will be combined (possibly by a Kalman filter or neural networks) to cancel out the correlated errors.

REFERENCES

[1] E D Kaplan, *Understanding GPS Principles and application.* Artech House Publishers.

[2] Timothy Pratt, Charles Bostian, Jeremy Allnutt "Satellite Communications" Second Edition, John Wiley & Sons, Inc.

[3] Kai Borre, D.M.A., Nicolaj Bertelson, Peter Rinder, Soren Holdt, Jenson, *A software defined GPS and GALILEO receiver, a single frequency approach.* 2006: Birkhauser.

[4] "GPS tutorial, Signals and data, Application Engineering", u Nav Microelctronics, USA.

[5] Public Release Version of "Navstar GPS User Equipment Introduction".

[6] Wells, D., N. Beck, D. Delikaraoglou, A. Kleusberg, E. Krakiwsky, G. Lachapelle, R. Langley, M. Nakiboglu, K. P. Schwarz, J. Tranquilla, P. Vanicek. (1987). *Guide to GPS Positioning*, 2nd printing with corrections, Canadian GPS Associates.

[7] Langley, R. (1996). *GPS for Geodesy, Chapter 5: GPS Receivers and Observables.* 2nd Edition, Springer-Verlag, pp. 151-185.

[8] Lachapelle, G., P. Kielland, and M. Casey: "GPS for Marine Navigation and Hydrography." International Hydrographic Review". Monaco, Vol. LXIX No. 1.

[9] Johan Malmstrom Robust "Navigation with GPS/INS and Adaptive Beamforming" Scientific Report, Swedish Defense Forces.

[10] Remondi, B. (1984): "Using the Global Positioning System (GPS) Phase Observable for Relative Geodesy: Modeling, Processing, and Results." Ph.D. Dissertation, Center for Space Research, The University of Texas at Austin, Austin.

[11] Thomas Pany, International Workshop on GPS Meteorology "Tropospheric GPS Slant Delays at Very Low Elevations" Institute for Geodesy and Navigation, University FAF Munich, Germany.

[12] Leick, A. (1995). *GPS Satellite Surveying.* John Wiley and Sons, Inc., 2nd edition.

[13] Klobuchar, J. A. (1987):" Ionospheric Time-delay Algorithm for Single-frequency GPS users". IEEE *Transactions on Aerospace and Electronic Systems,* Vol. AES-23, No. 2.

[14] Hopfield, H. (1971): "Tropospheric Effects on Electromagnetically Measured Range: Prediction from Surface Weather Data" Radio Science Vol.6 No. 3.

[15] Raquet, J. (1998). Development of a Method for Kinematic GPS Carrier-Phase Ambiguity Resolution Using Multiple Reference Receivers. PhD thesis, Department of Geomatics Engineering, University of Calgary, May.

[16] Lachapelle, G., A. Bruton, J. Henriksen, M. E. Cannon, and C. McMillan. "Evaluation of High Performance Multipath Reduction Technologies for Precise DGPS Shipborne Positioning". The Hydrographic Journal, Number 82, October, pp. 11-17.

[17] Seeber, G. (1993). *Satellite Geodesy Foundations, Methods, and Applications*. Published by Walter de Gruyter, pp. 291-295.

[18] Hopfield, H.S. (1969), "Two-quartic tropospheric refractivity profile for correcting satellite data", Journal of Geophysical Research, Vol. 74, No. 18, pp. 4487-4499.

[19] Saastamoinen, I. (1973). "Contribution to the Theory of Atmospheric Refraction". Bulletin Geodesique, No. 107, pp. 13-34.

[20] Edward E. Altshuler, "Tropospheric Range-Error Corrections for the Global Positioning System". IEEE Transactions on Antennas and Propagation, Vol. 46, No. 5, pp.643-649, May 1998.

[21] Theodore L. Beach,Paul M. Kintner, "Development and Use of a GPS Ionospheric Scintillation Monitor". IEEE Transactions on Geoscience and Remote Sensing, Vol. 39, No. 5, pp.918-928, May 2001.

[22] Siti Sarah Nik Zulkifli, Mardina Abdullah and Mahamod Ismail, "Application of 3-D Ray-Tracing for Accurate GPS Range Finding". The 5th Student Conference on Research and Development –SCOReD 2007 11-12 December 2007, Malaysia.

[23] Hagerman, L. L. (1973), "Effects of Multipath on Coherent and Noncoherent PRN Ranging Receiver." Aerospace Corporation Report No. TOR-0073(3020-03), 1973.

[24] Evans, A. (1986): "Comparison of GPS Pseudorange and Biased Doppler Range Measurements to Demonstrate Signal Multipath Effects." International Telemetering Conference, Las Vegas, NV.

[25] Georgiadou, Y., and A. Kleusberg, "On the Effect of Ionospheric Delay on Geodetic Relative GPS Positioning." Manuscripta Geodetica, Vol. 13, No. 13.

[26] Abidin, H. (1990): "Extra-widelanding for 1On the Fly' Ambiguity Resolution: Simulation of Multipath Effects." ION GPS-90, Colorado Springs, CO.

[27] Tajul A. Musa, et.al, "GPS Network-Based Approach to Mitigate Residual Tropospheric Delay in Low Latitude Areas", School of Surveying and Spatial Information Systems, The University of New South Wales, Sydney, NSW 2052, Australia.

[28] JiHong Zhang, "Investigations into the Estimation of Residual Tropospheric Delays in a GPS Network", MS thesis, 1999, Department of Geomatics Engineering, University of Calgary, Alberta, Canada.

[29] Hopfield, H.S. (1979), "Improvements in the tropospheric refraction correction for range measurement", Philosophical transactions of the Royal Society of London. Series A, 294, pp 341-352.

[30] M. Mainul Hoque, N. Jakowski, "Higher order ionospheric effects in precise GNSS positioning", Journal of Geodesy, (2007), Vol. 81, pp 259–268.

[31] S. Choy, et.al "An Evaluation of Various Ionospheric Error Mitigation Methods used in Single Frequency PPP", Journal of Global Positioning Systems (2008), Vol. 7, No. 1, pp: 62-71

[32] J.K.Ray, M.E.Cannon, "Mitigation of Static Carrier Phase Multipath Effects using Multiple Closely-Spaced Antennas". Presented at ION GPS-98, Nashville, September 15-18.

[33] Linlin Ge, et.al, "Multipath Mitigation of Continuous GPS Measurements using an Adaptive Filter", GPS Solutions, Vol. 4, No. 2, page 19-30 (2000).

[34] Calmin D. Scarlett, et.al. "Cellular based GPS Error Correction System". Proceedings, XVII IMEKO World Congress, June 22 – 27, 2003, Dubrovnik, Croatia.

[35] David Hadaller, "Mitigating GPS Error in Mobile Environments", Technical Report CS-2008-13 July 14, 2008, University of Waterloo.

[36] Sarawut Nontasud, Nipha Leelaruji. "Applied the artificial neural network to reduce the position error on GPS receiver due to ionospheric irregularities",

International Symposium on Communication and Information Technologies pp.647-651, 2008.

[37] Colombo, O. L. (1991), "Errors in Long Distance Kinematic GPS", In Proceedings of the 4th International Technical Meeting of the Satellite Division of the Institute of Navigation (ION GPS-91), pages 673–680. Albuquerque, New Mexico.

[38] Ehsani, M., Sullivan, M., Zimmerman, T., Stombaugh, T. "Evaluating the Dynamic Accuracy of Low-Cost GPS Receivers", ASAE Meeting Paper (2003).

[39] Wang Z., Wu Y., Zhang K. and Meng Y. (2004), "Triple Frequency Method for High-order Ionospheric Refractive Error Modeling in GPS Modernization", Journal of Global Positioning Systems, Vol. 4, No.1+2, pp. 291-295.

[40] Wu S., Yuan Y., Zhang K. and Grenfell R. (2006), "Temporal and Spatial Variations of the Ionospheric TEC over Victoria for GPSnet-based Real-time Positioning", Journal of Global Positioning Systems, Vol.5, No.1-2, pp.52-57.

[41] Zhang K.; Wu S. and Wu F. (2007), "The Latest Development of a Network-based RTK System in Australia", International Journal of Science and Research, Vol. 2(1), pp.87-94.

[42] Usman, M. "An Imaging System Based on the Combination of GPS (Global Positioning System) and SAR (Synthetic Aperture Radar)". 2006, The University of Manchester.

[43] Massat, P., and Rudnick, K., Geometric Formulas for Dilution of Precision Calculations. Navigation, 1990. 37(4): p. 379-391.

[44] Misra, P., and P. Enge, *Global Positioning System.* 2001, Ganga-Jumana Press.

[45] Goad, C.C. & Goodman, L. "A Modified Tropospheric Refraction Correction Model". Paper presented at the American Geophysical Union Annual Fall Meeting, San Francisco, December 12-17, 1974.

International Islamic Univ.
CENTRAL
LIBRARY
ISLAMABAD.